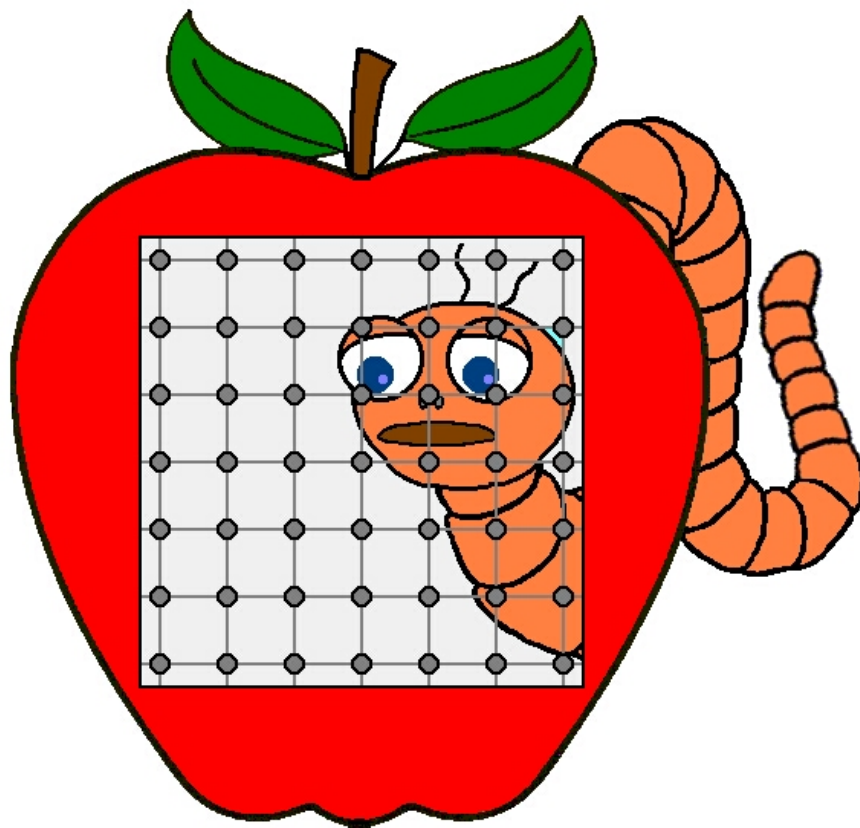


# 54th MIDWEST SOLID STATE CONFERENCE

University of Nebraska, Lincoln, NE 68588

October 6-7, 2007



## **Sponsored by**

Nebraska Center for Materials and Nanoscience

Department of Physics and Astronomy

The Office of the UNL Vice Chancellor for Research

College of Arts and Sciences



# General Information

*Date:* October 6-7, 2007

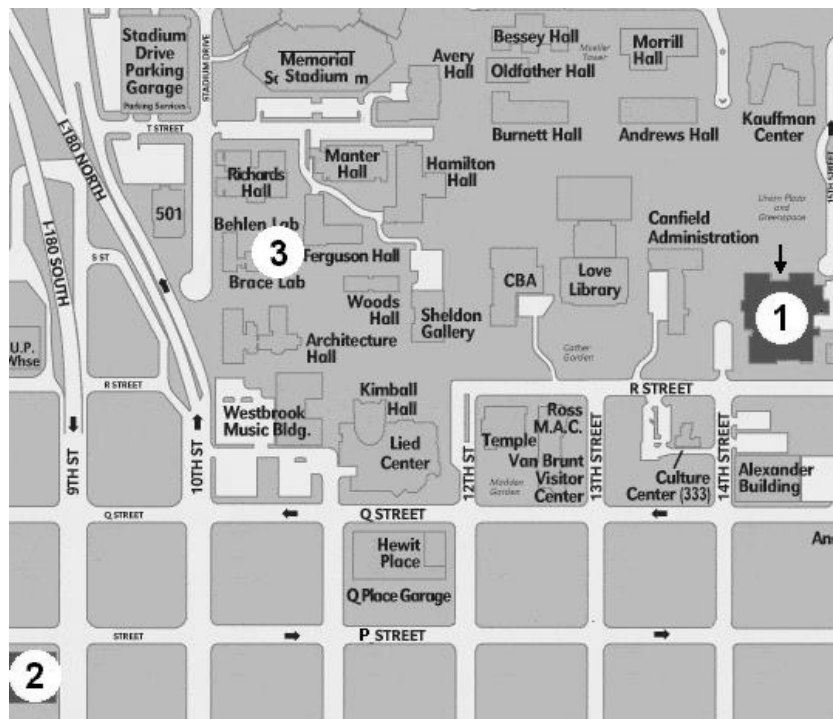
*Location:* Nebraska Union Auditorium, 14th & R Street, Lincoln, NE 68588  
(Follow arrow above Point 1 in map and use spiral stairs)

*Organization Committee*

Sitaram Jaswal (Chair)  
Sy-Hwang Liou  
Ralph Skomski

*Conference Secretary:*

Verona Skomski (vskomski3@unl.edu)



1 Nebraska Union, 2 Holliday Inn, 3 Department of Physics and Astronomy

**COVER PAGE: Newton's Worm**

On UNL campus, near the physics building, there is an apple tree grafted from Newton's original source of knowledge. Little was known in the 17th century about the internal structure and physics of solids. — Have you noticed that apples hardly crystallize in a cubic structure? That's why the worm is so surprised!



# Conference Program

**Saturday, October 6**

8:00-12:00    **Registration**    **Auditorium Lobby**

8:00-8:45    **Continental Breakfast**    **Ballroom**

**Opening of Conference and Plenary Session**    **Auditorium**

*(Chair: Sitaram S. Jaswal)*

8:45-9:00    Welcome remarks by David Sellmyer, Director, Nebraska Center for Materials and Nanoscience, and Prem Paul, Vice Chancellor for Research

9:00-10:00    Prof. Lu J. Sham; University of California San Diego  
"Quantum Engineering of Individual Electron Spins"

10:00-10:30    **Coffee Break**    **Ballroom**

**Session A**    *Chair: Steve Ducharme*    **Auditorium**

10:30-11:00    A.1: Steve Smith, South Dakota School of Mines and Technology  
"Near-Field Spectral Imaging of Solar Cell Materials"

11:00-11:30    A.2: Owen Vajk, University of Missouri - Columbia  
"Experimental Signatures of Magnetic-Ferroelectric Coupling from Neutron Scattering"

11:30-12:00    A.3: Hongxing Jiang, Kansas State University  
"Nitride Micro- and Nano-Photonics"

12:00-1:00    **Lunch + Poster Session Preparation**    **Ballroom**

**Session B**    *Chair: Ralph Skomski*    **Auditorium**

1:00-1:30    B.1: Walter Lambrecht, Case Western Reserve University  
"Magnetic and Electronic Properties of Transition-Metal and Rare-Earth Nitrides"

1:30-2:00    B.2: Axel Enders, University of Nebraska - Lincoln  
"Growth and Magnetism of Surface-Supported Metallic Nanoclusters"

2:00-2:30    B.3: Andre G. Petukhov, South Dakota School of Mines and Technology  
"Thermodynamics of Carrier-Mediated Magnetism in Semiconductors"

2:30-3:00	B.4: Viatcheslav V. Dobrovitski, Iowa State University "Quantum Spin Dynamics and Decoherence in Nanosystems"	
3:00-6:30	<b>Poster Sessions P-S</b> (Chair: <i>Sy-Hwang Liou</i> , Co-Chair: <i>Christian Binek</i> )	<b>Ballroom</b>
3:00-3:30	Coffee Break	<b>Ballroom</b>
5:00-6:30	Bierstube	<b>Ballroom</b>
6:30-8:00	Banquet	<b>Ballroom</b>
8:00	Performance: Kokyo Taiko Drummers	<b>Ballroom</b>

### **Sunday, October 7**

8:00-9:00	<b>Continental Breakfast</b>	<b>Lobby Auditorium</b>
-----------	------------------------------	-------------------------

<b>Session C</b>	Chair: <i>Evgeny Tsymbal</i>	<b>Auditorium</b>
------------------	------------------------------	-------------------

9:00-9:30 C.1: Anupam Garg, Northwestern University  
"Collective Spin Tunneling in Magnetic Molecules"

9:30-10:00 C.2: Hui Zhao, University of Kansas  
"Optical Studies of Ballistic Pure Spin Transport"

10:00-10:30 C.3: Michael E. Flatté, University of Iowa  
"Single-Ion Magnetic Moments in Semiconductors"

10:30-10:45	<b>Coffee Break</b>	<b>Lobby Auditorium</b>
-------------	---------------------	-------------------------

<b>Session D</b>	Chair: <i>Shireen Adenwalla</i>	<b>Auditorium</b>
------------------	---------------------------------	-------------------

10:45-11:15 D.1: Wai-Yim Ching, University of Missouri - Kansas City  
"Ab initio Calculations on Complex Biomolecular Systems"

11:15-11:45 D.2: Maikel Rheinstädter, University of Missouri -Columbia  
"Impact of Neutrons on the Understanding of Dynamics in Soft-Matter and Biophysics"

11:45-12:00 **Closing Session**  
(Chair: *Sitaram S. Jaswal*)

## Poster Sessions

### Session P: Theory

- P.1 “Phase Transitions in Quantum Ring and Sphere Arrays”  
Kieran Mullen, Bahman Roostaei, and Ethan Brown
- P.2 “Effect of Magnetic Short-range Order on Spin-disorder Resistivity”  
A. L. Wysocki, K. D. Belashchenko, M. van Schilfgarde, J. P. Velev
- P.3 “Thermodynamics of Itinerant Magnets: A Simple Classical Model with Longitudinal Spin Fluctuations”  
A. L. Wysocki, J. K. Glasbrenner, and K. D. Belashchenko
- P.4 “The Origins of Tunneling Anisotropic Magnetoresistance in Nanoscale Ferromagnetic Metal Break Junctions”  
J. D. Burton, R. F. Sabirianov, J. P. Velev, O. N. Mryasov, and E. Y. Tsymbal
- P.5 “Surface Induced Suppression of Magnetization in Nanoparticles”  
C. Westman, S. Jang, C. Kim, S. He, G. Harmon, N. Miller, B. Graves, N. Poudyal, R. Sabirianov, H. Zeng, M. DeMarco, and J. P. Liu
- P.6 “Surface Finite Size Effect in Nanoparticles”  
J. Koch and Renat Sabirianov
- P.7 “Electronic Properties of LaB<sub>6</sub>: a Theoretical Study”  
Guangping Li, Jing Lu, R. Sabirianov, Wai-Ning Mei, C. L. Cheung, and X. C. Zeng
- P.8 “Analytical and Numerical Solution of Double Well Using Triconfluent Heun Function”  
A. Holloway, W.N. Mei, and R.F. Sabirianov
- P.9 “Mullite: Structure and Properties”  
Sitaram Aryal, Hongzhi Yao, and W. Y. Ching
- P.10 “Theoretical ELNES/XANES Spectroscopic Study of a  $\Sigma 5$  Grain Boundary Model in SrTiO<sub>3</sub>”  
Paul Rulis and W. Y. Ching
- P.11 “First-principles Investigations of the Electronic Structure and Magnetic Properties of Fe<sub>3</sub>O<sub>4</sub>(001)/MgO(001) Interface”  
Hongzhi Yao, Lizhi Ouyang, and W. Y. Ching
- P.12 “Electronic Structure of B-DNA Models”  
L. Liang, Paul. Rulis, and W-Y. Ching
- P.13 “First-principles Calculation of MCD for Cr *L*<sub>2,3</sub>-edge XANES of CrO<sub>2</sub>”  
Kazuyoshi Ogasawara and Sachiyo Kiyozumi
- P.14 “The Harris Criterion and disordered 3D Heisenberg Models”  
Donald J. Priour, Jr.
- P.15 “Modeling the FQHE from First Principles”  
M. L. Horner and Alfred Scharff Goldhaber

## Session Q: Magnetism

- Q.1 “The Electronic Band Structure of  $\text{CoS}_2$ ”  
Ning Wu, Ya.B. Losovyj, David Wisbey, K. Belashchenko, L. Wang, M. Manno, C. Leighton, and P.A. Dowben
- Q.2 “Proteresis in Co:CoO Core-Shell Nanoclusters”  
X.-H. Wei, R. Skomski, Z.-G. Sun, and D. J. Sellmyer
- Q.3 “Magnetization Precession and Damping in Ni/Pt Bilayers”  
Steven Michalski and Roger Kirby
- Q.4 “ $\text{L}_{10}$  FePt:X Films”  
Tom A. George, Zhen Li, Minglang Yan, Yingfan Xu, Ralph Skomski, and David J. Sellmyer
- Q.5 “Texture Development and Magnetic Properties of Ru-doped FePt Films”  
Zhen Li, Yucheng Sui, Lanping Yue, Roger D. Kirby, David J. Sellmyer
- Q.6 “Scaling Behavior of the Exchange Bias Training Effect”  
Srinivas Polisetty, Sarbeswar Sahoo, and Christian Binek
- Q.7 “Method to Create Cubic FePt Clusters During *in situ* Gas-Phase Aggregation”  
M. M. Patterson, X. Rui, J. Shield, and D. J. Sellmyer
- Q.8 “Photoconductive Circuit for the Study of Magnetization Precession”  
Robert Mumgaard, Bob Buckley, Steven Michalski, and Roger Kirby
- Q.9 “Generalized Magneto-optic Ellipsometry on  $\text{Zn}_{1-x}\text{Mn}_x\text{Se}$ : Dielectric and Magnetic Induced Optical Anisotropy”  
M. Saenger, B. Daniel, M. Hetterich, T. Hofmann, and M. Schubert
- Q.10 “Magnetocaloric Properties of Co/Cr Multilayers”  
T. Mukherjee, S. Sahoo, R. Skomski, D. J. Sellmyer, and Ch. Binek
- Q.11 “Advanced MFM Probes for Magnetic Domain Imaging of both Hard and Soft Magnetic Films”  
L. Nicholl, R. Zhang, S. H. Liou, L. Yuan, D. Pappas, and Bao Shan Han
- Q.12 “Study of Noise in Magnetic Tunneling Junction Sensors with a 64-elements Symmetric Bridge”  
R. Zhang S. H. Liou, Stephen E. Russek, L. Yuan, S. T. Halloran, and D. P. Pappas

## Session R: Ferroelectric and Multiferroic Systems

- R.1 “Magneto-Electric Coupling in Ferromagnetic Cobalt/Ferroelectric Copolymer Multi-Layer Films”  
A. Mardana, M. Bai, A. Baruth, T. Reece, S. Ducharme, and S. Adenwalla
- R.2 “Electroresistance in Ferroelectric Tunnel Junctions with Asymmetric Polar Interfaces”  
J. Snodgrass and R. F. Sabirianov

- R.3 “Synthesis of the Giant Dielectric Constant Material  $\text{CaCu}_3\text{Ti}_4\text{O}_{12}$  by Wet-Chemistry Methods”  
Jianjun Liu, Robert W. Smith, and Wai-Ning Mei
- R.4 “Piezomagnetic Effect in Mn-Based Antiperovskites”  
Pavel Lukashev and Renat Sabirianov
- R.5 “Electron Transport in Ferroelectric and Multiferroic Tunnel Junctions”  
Julian P. Velev, Chun-Gang Duan, Kirill D. Belashchenko, Sitaram S. Jaswal, and Evgeny Y. Tsymbal
- R.6 “Ferroelectric Control of Magnetism in  $\text{BaTiO}_3/\text{Fe}$  Heterostructures”  
Srinivas Polisetty, Sarbeswar Sahoo, Chun-Gang Duan, Sitaram S. Jaswal, Evgeny Y. Tsymbal, and Christian Binek
- R.7 “Magnetic and Magnetoelectric Properties of Epitaxial  $\text{Cr}_2\text{O}_3$  Thin Films”  
Xi He, Yi Wang, Sarbeswar Sahoo, and Christian Binek
- R.8 “Magnetism of  $\text{LaAlO}_3/\text{SrTiO}_3$  Superlattices”  
Karolina Janicka, Julian P. Velev and Evgeny Y. Tsymbal
- R.9 “Structure of Langmuir-Blodgett Films of Vinylidene Fluoride Oligomers”  
Yong Wang, Jihee Kim, Nick Reding, Kristin Kraemer, Stephen Ducharme, Zhongxin Ge, and James M. Takacs
- R.10 “Modeling the Small Signal Capacitance-Voltage Characteristics of Metal-Ferroelectric-Insulator-Memory Elements Based on Langmuir-Blodgett Copolymer Films”  
T. J. Reece and Stephen Ducharme
- R.11 “Locally Probed Ferroelectricity of Ferroelectric Nanomesas by Piezoresponse Force Microscopy”  
Jihee Kim, Stephen Ducharme, Brian Rodriguez, Stephen Jesse, and Sergei V. Kalinin
- R.12 “Spectroscopic and Density Functional Theory Studies of Vinylidene Fluoride Oligomers”  
J. Travis Johnston, Jihee Kim, Rafal Korlacki, Stephen Ducharme, Zhongxin Ge, and James M. Takacs
- R.13 “Apparatus for Pyroelectric Scanning Microscopy”  
Stella Stephens, Horatio Vasquez, Jihee Kim, and Stephen Ducharme
- R.14 “Effect of Ferroelectric Polarization on Tunneling Current”  
Evgeny Kiriranov, Jody Redepinning, and Andrei Sokolov

### **Session S: Semiconductors and Special Topics**

- S.1 “Activated Water Desorption from Poly(vinylidene fluoride with trifluoroethylene) and Poly(methylvinylidene cyanide)”  
Carolina C. Ilie, P. A. Jacobson, I. N. Yakovkin, Luis. G. Rosa, Jie Xiao, Matt Poulsen, D. Sahadeva Reddy, James M. Takacs, P. A. Dowben

- S.2 “Stabilizer-free Nanostructured Zirconia”  
Gonghua Wang, Chin Li Cheung, Fereydoon Namavar, Jaeil Bai, Renat F. Sabirianov, Xiao Cheng Zeng, Joseph R. Brewer, Wai -Ning Mei, Hani Haider, and Kevin L. Garvin
- S.3 “Polarized and Time-resolved Photoluminescence Measurements of Single Zincblende and Wurzite InP Nanowires”  
J. M. Yarrison-Rice, A. Mishra, T.B. Hoang, L.V. Titova, L.M. Smith, H.E. Jackson, H.J. Joyce, H.H. Tan, and C. Jagadish
- S.4 “Investigation of Single CdS Nanosheets with Spatially-, Temporally-, and Polarization-resolved Photoluminescence”  
H. E. Jackson, K.-Y. Lee, H. Rho, L. V. Titova, T. B. Hoang, A. Mishra, L. M. Smith, J. M. Yarrison-Rice, Y.-J. Choi, K.-J. Choi, and J.-G. Park
- S.5 “Growth of Crystalline Lanthanum Hexaboride Nanostructures”  
Joseph R. Brewer, Nirmalendu Deo, and Chin Li Cheung
- S.6 “The Elastic Constants and Related Mechanical Properties of the Monoclinic Polymorph of the Carbamazepine Molecular Crystal”  
Himansu Mohapatra and Craig J. Eckhardt
- S.7 “The Role of Defects in Amorphous Hydrogenated Boron Carbide  $\alpha$ -B<sub>5</sub>C:H”  
M. Sky Driver and A. N. Caruso
- S.8 “The Bulk Band Structure and Inner Potential of Layered In<sub>4</sub>Se<sub>3</sub>”  
Jing Liu, Ya. B. Losovyj, T. Komesu, P. A. Dowben, L. Makinistian, E. A. Albanesi, Andre Petukhov, P. Galiy, and Ya. Fiyala
- S.9 “Comparison of Electric Properties of Boron Carbide and N-Doped Boron Carbide”  
Nina Hong, Ravi Billa, and Shireen Adenwalla
- S.10 “Nd<sup>3+</sup>-Doped Titania Nanotubes”  
Wanwan Huang, Dilip K. Paul, and Chin Li Cheung
- S.11 “Polarization Coupled Response of ZnO-BaTiO<sub>3</sub> Heterojunctions: A Model Approach”  
V. M. Voora, T. Hofmann, M. Brandt, M. Lorenz, M. Grundmann, and M. Schubert
- S.12 „Angle-Resolved Generalized Ellipsometry: Form-Birefringent Chiral and Achiral Silicon Sculptured Thin Films”  
D. Schmidt, E. Schubert, and M. Schubert
- S.13 “Nanoscale Observation of Delayering in Alkane Films”  
M. Bai, K. Knorr, H. Taub, U. G. Volkmann, and F. Y. Hansen
- S.14 “Studies of the Dynamics of Alkane Nanoparticles”  
S.-K. Wang, M. Bai, H. Taub, J. R. D. Copley, V. Garcia Sakai, G. Gasparovic, M. Rheinstädter, U. G. Volkmann, and F. Y. Hansen
- S.15 “Temperature Dependent Dielectric Function of Al<sub>0.52</sub>In<sub>0.48</sub>P and Ga<sub>0.52</sub>In<sub>0.48</sub>P”  
E. Montgomery, T. Hofmann, and M. Schubert

# Plenary Talk:

## Quantum Engineering of Individual Electron Spins

**L. J. Sham**

*Department of Physics, University of California San Diego, La Jolla, CA 92093-0319*  
*E-mail: lsham@ucsd.edu*

The key issues

- As the devices go nano, quantum engineering takes over; resistance is futile.
- How to build an isolated quantum system. In our case, how to trap an electron [1].
- Preparation of a quantum state, its transformation and measurement are issues of interaction between the macro and the micro systems. Both theory and experiment will be covered [2-7].
- The deleterious effects of the environment. Can they be avoided or reversed? [8-10]
- How to scale from the laboratory system of one or two quantum units to a large number (increasing the unit number without exponential increase in resource). A solution with a solid state quantum network of nodes and waveguides [11,12].

*Acknowledgment.* This talk is based on the work of the collaboration of Dan Gammon and his group at Naval Research Laboratory, Duncan Steel and his group at the University of Michigan, and my theory collaborators. Some of their names are in the reference list. I am also indebted to ARO/NSA-LPS, DARPA-QuIST, and NSF DMR for their financial support.

### References

- [1] E. A. Stinaff, M. Scheibner, A. S. Bracker, I. V. Ponomarev, V. L. Korenev, M. E. Ware, M. F. Doty, T. L. Reinecke, D. Gammon, "Optical Signatures of Coupled Quantum Dots", *Science* **311**, 636 (2006).
- [2] C. Emary and L. J. Sham, "Optically controlled single-qubit rotations in self-assembled InAs quantum dots", *J. Phys.: Condens. Matter* **19**, 056203, (2007).

- [3] C. Emary, X.-D. Xu, D. G. Steel, S. Saikin, L.J. Sham, "Fast initialization of the spin state of an electron in a quantum dot in the Voigt configuration," *Phys. Rev. Lett.* **98**, 047401 (2007).
- [4] Xi.-D. Xu, Y.-W. Wu, B. Sun, Q. Huang, J. Cheng, D. G. Steel, A. S. Bracker, D. Gammon, and C. Emary, L. J. Sham, "Fast Spin State Initialization in a Singly-Charged Quantum Dot," *Phys. Rev. Lett.*, in press (2007).
- [5] Y.-W. Wu, E. D. Kim, X.-D. Xu, J. Cheng, D. G. Steel A. S. Bracker, D. Gammon, S. Economou, and L. J. Sham, "Selective Optical Control of Electron Spin Coherence in Singly Charged Quantum Dots via Oscillating Dark and Bright States," *Phys. Rev. Lett.*, in press (2007).
- [6] X.-D. Xu, B. Sun, P. R. Berman, D. G. Steel, A. Bracker, D. Gammon, L. J. Sham, "The Mollow Spectrum and Gain in a Single Quantum Dot," *Science* **317**, 929 (2007).
- [7] C. Emary and L. J. Sham, "Optically controlled logic gates for two spin qubits in vertically coupled quantum dots", *Phys. Rev. B* **75**, 125317 (2007).
- [8] W. Yao, R.-B. Liu, and L. J. Sham, "Theory of electron spin decoherence by interacting nuclear spins in a quantum dot", *Phys. Rev. B* **74**, 195301 (2006).
- [9] W. Yao, R.-B. Liu, and L. J. Sham, "Restoring Coherence Lost to a Slow Interacting Mesoscopic Spin Bath", *Phys. Rev. Lett.* **98**, 077602 (2007). Publisher's Note: *Phys. Rev. Lett.* **98**, 077602 (2007).
- [10] R.-B. Liu, W. Yao and L. J. Sham, "Control of electron spin decoherence caused by electron–nuclear spin dynamics in a quantum dot". *New J. Phys.* **9**, 226 (2007). doi:10.1088/1367-2630/9/7/226
- [11] W. Yao, R.-B. Liu, and L. J. Sham, "Theory of Control of the Spin-Photon Interface for Quantum Networks", *Phys. Rev. Lett.* **95**, 030504 (2005).
- [12] R.-B. Liu, W. Yao, and L. J. Sham, "Coherent control of cavity quantum electrodynamics for quantum nondemolition measurements and ultrafast cooling", *Phys. Rev. B* **72**, 081306 (R) (2005).

**ABSTRACTS**  
**(INVITED PRESENTATIONS)**



# Near-Field Spectral Imaging of Solar Cell Materials

Steve Smith<sup>†,\*</sup>

<sup>\*</sup>South Dakota School of Mines and Technology, Rapid City, SD 57701 USA  
E-mail: Steve\_Smith@mailaps.org

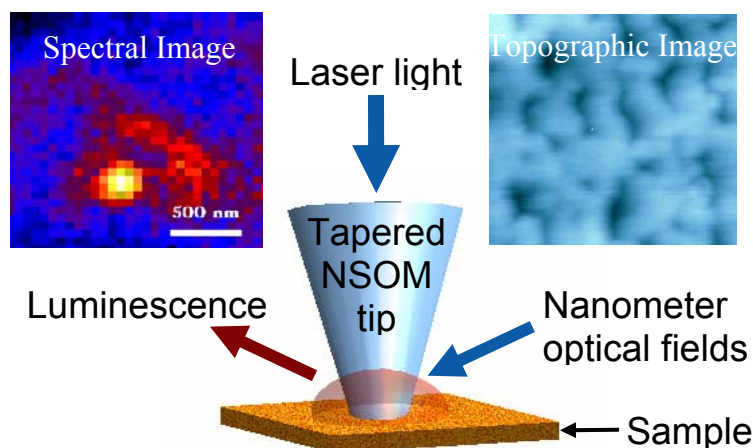


**Figure 1:** Laser light is confined spatially by a tapered optical fiber (typically 100nm). Luminescence is locally excited and analyzed, single excitons are spatially-spectrally isolated and their relation to structure in a semiconductor alloy is revealed.

We use aperture-based near-field microscopy and spectroscopy to spatially-resolve the luminescent constituents in solar cell materials. Two materials which are important to current and future solar cell technologies are the III-V GaInP, and the II-VI CdTe. Localized spectroscopy is used to identify electronic processes, and their relation to structure [1-3]. Figure 1 shows an example of this work: Both scanning and fixed-aperture near-field methods were employed at cryogenic temperatures and magnetic fields up to 5T, to investigate GaInP alloys. These bulk alloys exhibit naturally occurring quantum confined states, with the following signatures: reduced thermal broadening, exciton transfer among spatially- and energetically-neighboring localized states, reduced diamagnetic shift, and a mixture of long-lived, ostensibly indirect transitions, and nanosecond direct transitions. Work in progress focuses on implementing an apertureless near-field microscope [4] utilizing tunable femtosecond laser sources, with the intent of investigating multi-photon processes for so-called 3<sup>rd</sup> generation solar cell materials, in particular intermediate band materials to enhance solar cell efficiency [5-7].

- [1] S. Smith *et. al.*, *Mat. Res. Society Spring Meeting*, San Francisco, CA, Mar. 29th (2005).
- [2] S. Smith, P. Zhang, T. Gessert, and A. Mascarenhas, *Appl. Phys. Lett.* **85**, 3854 (2004).
- [3] S. Smith, A. Mascarenhas, S. P. Ahrenkiel, *et. al.*, *Phys. Rev. B* **68**, 035310 (2003).
- [4] E. Sanchez, L. Novotny, X.S. Xie, *Phys. Rev. Lett.* **82** 4014 (1999).
- [5] A. Luque and A. Martí, *Phys. Rev. Lett.* **78** 5014 (1997); *ibid* (PRL) **97**, 247701 (2006).
- [6] R. W. Peng, M. Mazzer, K. W. J. Barnham, *Appl. Phys. Lett.* **83** 770 (2003).
- [7] K. M. Yu *et. al.* *Phys. Rev. Lett.* **91**, 246403 (2003); *proc. Mat. Res. Soc.* **865** F5.7.1 (2005).

<sup>†</sup>Some work performed while at NREL, Golden, CO 80401

## **Experimental Signatures of Magnetic-Ferroelectric Coupling from Neutron Scattering**

**Owen Vajk**

*Department of Physics and Astronomy, University of Missouri-Columbia  
E-mail: vajko@missouri.edu*

Materials with simultaneous ferroelectric and magnetic order, so-called multiferroics, have attracted attention because of the possibility of using magnetic fields to affect ferroelectric order or electric fields to affect magnetic order. Such magneto-electric susceptibility requires coupling between the two order parameters, which has only been observed in a relatively small class of materials. Theoretical understanding of the coupling mechanisms in these materials is still lacking, and may not be possible without more guidance from experiments. This talk will present some evidence for possible coupling mechanisms from neutron scattering measurements on multiferroic materials.

## Nitride Micro- and Nano-Photonics

**Hongxing Jiang**

*Kansas State University, Manhattan, KS*

*E-mail: [jiang@phys.ksu.edu](mailto:jiang@phys.ksu.edu)*

A brief overview on recent advances in the area of micro- and nano-photonic structures and devices based upon III-nitride wide bandgap semiconductors will be presented. Exploitation of chip-level innovation and integration of nitride photonic devices will be reviewed. Three potential applications of nitride nanophotonics will be discussed, including nitride photonic crystals (PCs) for enhancing power output of blue/green/white LEDs for solid state lighting, Er doped nitride photonic structures for optical communications, and nitride quantum wells and superlattices as thermoelectric (TE) materials for directly converting waste heat to electricity.

# Magnetic and Electronic Properties of Transition-Metal and Rare-Earth Nitrides\*

Walter R. L. Lambrecht

*Department of Physics, Case Western Reserve University, Cleveland OH 44106-7079  
E-mail: walter.lambrecht@case.edu*

Transition metal and rare-earth nitrides present a wide variety of magnetic and electronic properties, from antiferromagnetic semiconductors to ferromagnetic metals. We have started exploring some of these materials with first-principles calculations to shed light on the origins of magnetic behavior in this family of materials. In this talk, I will focus on a few systems of particular interest. The first example is Mn doped ScN [1]. ScN is a non-magnetic semiconductor and the goal behind this work is to explore if it could be a host for a dilute magnetic semiconductor (DMS). We use the linear response Green's function approach to calculate the exchange interactions in this system. We find the existence of long-range interactions. The effects of doping, disorder and band gap corrections in ScN are investigated. Critical temperatures were calculated using a recently proposed generalization of the cluster variation method. We predict an increase of the critical temperature with Mn concentration which saturates at about 400K for concentrations of about 25 % which are easily achievable in this system. Our second example is rare-earth nitrides. In this case, we used the LSDA+U approach to treat the strongly correlated f-electrons. It was found that the cubic symmetry in this system is broken by the formation of orbital magnetic moments, following Hund's rule in most cases [2]. The question of whether these materials are semiconductors or semimetals will be discussed in the context of recent experiments on GdN. Recent optical studies by the group of J. Trodahl show clear evidence of a gap, which redshifts below the Curie temperature but semiconducting behavior is still observed in the ferromagnetic state. We discuss how this can be simulated by adding a  $U_d$  in the LSDA+U approach but caution that the underlying physics here is different. In these materials, energy differences between different magnetic configurations can be mapped on a Heisenberg Hamiltonian with only first and second nearest neighbor interaction and this model is shown to successfully account for the trends in magnetic properties of the Gd group-V compound series [3] and the Eu-chalcogenides [4].

- \*Work done in collaboration with A. Herwadkar, P. Larson, M. S. Miao, P. Lukashev, C. Mitra, M. van Schilfgaarde, A. Chantis, A. Preston, J. Trodahl, B. Ruck, K. Smith
- Funded by NSF, ONR and ARO.

## References

- [1] A. Herwadkar and W. R. L. Lambrecht, Phys. Rev. B **72**, 235207 (2005).  
 [2] P. Larson et al., Phys. Rev. B **75**, 045114 (2007).  
 [3] P. Larson and Walter R. L. Lambrecht, Phys. Rev. B **74**, 085108 (2006).  
 [4] P. Larson and Walter R. L. Lambrecht, J. Phys. Condens. Matter **18**, 11333 (2006).

# Growth and Magnetism of Surface-Supported Metallic Nanoclusters

**A. Enders**

*University of Nebraska, Lincoln, NE 68588-0111, USA, and  
Max Planck Institute for Solid State Research, 70569 Stuttgart, Germany  
E-mail: aenders2@unl.edu*

It is generally recognized that the fabrication of magnetic storage media with bit densities of Gigabytes per square inch and more is out of reach of currently available thin film technologies. Patterned media may therefore set off to challenge thin film media as they allow in principle for bit densities several orders of magnitude larger than what is currently feasible. In this talk I will show how spherical clusters of less than 2 nm diameter can be fabricated on substrates directly by self-assembled growth using noble gas buffer layers. The resulting clusters are randomly distributed over the bare substrate surface. The magnetism of such clusters, studied with X-ray magnetic circular dichroism, shows strong dependence on the substrate material. On Pt, for instance, the preferential magnetization direction is out-of-plane, while it is in-plane on Ag. The application of self-assembled clusters as individually addressable magnetic units requires their controlled arrangement into well-defined ordered arrays. We are therefore guiding the clusters with energetic sinks provided by periodic network structures prefabricated on the substrate. We use mechanically extremely stable boron nitride nanomesh monolayers as template surfaces. We will demonstrate that densely packed ordered cluster layers are achieved by repeated cluster deposition cycles. The magnetic properties of the cluster ensemble as well as the application of the mesh as reactor for the fabrication of ordered, binary alloy clusters will be discussed.

# Thermodynamics of Carrier-Mediated Magnetism in Semiconductors

A. G. Petukhov<sup>1</sup>

*Department of Physics, South Dakota School of Mines and Technology,  
Rapid City, SD 57701*

*E-mail: Andre.Petukhov@sdsmt.edu*

We propose a model of carrier-mediated ferromagnetism in semiconductors that accounts for the temperature dependence of the carriers [1]. The model permits analysis of the thermodynamic stability of competing magnetic states, opening the door to the construction of magnetic phase diagrams. As an example we analyze the stability of a possible reentrant ferromagnetic semiconductor, in which increasing temperature leads to an increased carrier density, such that the enhanced exchange coupling between magnetic impurities results in the onset of ferromagnetism as temperature is raised.

[1] A. G. Petukhov, I. Zutic, and S. C. Erwin, ArXiv: cond-mat/0705.4464v1.

---

<sup>1</sup> In collaboration with I. Zutic (SUNY Buffalo) and S.C. Erwin (NRL). Supported by US ONR.

# Quantum Spin Dynamics and Decoherence in Nanosystems

**Viatcheslav V. Dobrovitski**

*Ames Laboratory and Iowa State University, Ames, IA, 50014  
E-mail: slava@ameslab.gov*

Harnessing quantum coherence of electron and/or nuclear spins for new applications is an interesting research endeavor, holding much promise for high-precision metrology, coherent spintronics, and quantum information processing. However, progress in these areas is limited, because quantum coherence is easily destroyed by interaction with environment. This decoherence phenomenon, being of fundamental importance, is currently under active investigation.

The presentation is focused on our recent theoretical studies of quantum spin dynamics and decoherence in some experimentally interesting systems and their environments, such as electron spins in quantum dots, nuclear spins in solid-state NMR systems, etc.[1] Decoherence is a complex non-equilibrium many-body quantum process, and numerical simulations present a valuable tool for describing and understanding decoherence dynamics. We will discuss advanced numerical approaches to decoherence modeling, both exact and approximate, which can be used for efficient and accurate simulations of the systems comprising tens to thousands of quantum spins. We will show how our newly developed techniques can be applied to investigation of non-trivial decoherence regimes which are difficult to study analytically (such as the unusual logarithmic decay of the electron spin in a quantum dot decohered by a nuclear spin bath). Moreover, the numerical simulations play an important role in analyzing various quantum control protocols designed for suppressing decoherence in spin systems. Our recent results on performance of various deterministic and randomized quantum control protocols will be presented, focusing on the experimentally interesting regimes where existing simplified analytical approaches are not applicable. We will show how specially designed protocols can increase the coherence time by orders of magnitude, and in some cases, even completely “freeze” decoherence [2].

The presentation is based on a number of works supported by DOE, NSA and ARO.

## References

- [1] W. Zhang, N. Konstantinidis, K. A. Al-Hassanieh, and V. V. Dobrovitski, “Modeling decoherence in quantum spin systems” (topical review), *J. Phys.: Cond. Matter* **19**, 083202 (2007).
- [2] W. Zhang, V. V. Dobrovitski, L. F. Santos, L. Viola, and B. N. Harmon, “Dynamical control of electron spin coherence in a quantum dot: A theoretical study”, *Phys. Rev. B* **75**, 201302 (R) (2007).

# Collective Spin Tunneling in Magnetic Molecules

**Anupam Garg**

*Department of Physics and Astronomy  
Northwestern University, Evanston, IL 60208  
E-mail: [agarg@northwestern.edu](mailto:agarg@northwestern.edu)*

Several molecular solids ( $\text{Fe}_8\text{-tacn}$ ,  $\text{Mn}_{12}$  derivatives) have now been seen to display spin tunneling, through the dramatic phenomenon of splitting oscillations. The magnetic complex in each solid has a large spin (10 or 9.5), and a local Ising type anisotropy, so the spin orientation can tunnel from "up" to "down". If a static magnetic field  $H$  is applied along the hard axis, the tunnel splitting oscillates as a function of  $H$ , being quenched at specific magnetic field values.

The quenching of tunneling can be understood in terms of interfering semiclassical spin paths in a path integral view. The spin path integral is mathematically delicate, however; the spin paths may even be discontinuous, for example. Such paths must be included for  $\text{Fe}_8$ , and once this is done we obtain excellent agreement between theory and experiment. The  $\text{Fe}_8$  experiments have thus provided a major impetus for work on spin path integrals.

The measurements of the tunnel splitting are done by an innovative application of the Landau-Zener-Stuckelberg protocol. While the general phenomenon of splitting oscillations is unambiguously observed, a full understanding of LZS in the context of magnetic molecular solids requires inclusion of decoherence effects and the large and long-ranged dipole-dipole interaction between different molecules. This is a challenging and only partially solved problem at present.

Work supported by NSF Grant DMR-0202165.

# Optical Studies of Ballistic Pure Spin Transport

Hui Zhao<sup>1</sup> and Arthur L. Smirl<sup>2</sup>

<sup>1</sup>*Department of Physics and Astronomy, The University of Kansas, Lawrence, KS 66045*

*E-mail: huizhao@ku.edu*

<sup>2</sup>*Lab for Photonics and Quantum Electronics, University of Iowa, Iowa City, IA 52242*

*E-mail: art-smirl@uiowa.edu*

Recently, there has been a growing interest in using the spin of electrons in addition to, or in place of, charge in semiconductor electronic devices. Spintronic devices are regarded as one of the most promising candidates for the next generation of electronics. Spin transport in semiconductors is a fundamental process in almost all spintronic devices.

We review our recent investigations of ballistic pure spin transport in GaAs quantum wells by using ultrafast laser techniques with high spatial and temporal resolution. In contrast to most spin-transport experiments carried out in diffusive regimes over large spatial scales, our recent studies have focused on the ballistic transport regime, where the length scales are comparable to or smaller than the mean-free-path of electrons [1]. By taking advantage of the quantum interference between the interband transition amplitudes for one-photon absorption and two-photon absorption, we can control the density and spin of excited electrons in momentum space. For example, by choosing the proper configurations of laser polarizations and phases, we can excite electrons to the conduction band such that electrons with spin  $+1/2$  preferentially occupy states with one sign of momenta, while electrons with spin  $-1/2$  are excited to the states with opposite momenta. This produces a net spin current, without introducing any net charge current or net spin polarization, a so called pure spin current. The ballistic transport of spin is observed in real space and real time by using highly sensitive pump-probe techniques with temporal resolution of 200 femtosecond and spatial resolution of less than 1 nanometer [1]. The direct measurement of ballistic spin transport over  $\sim 100$  nanometers provides information on fundamental parameters for spintronic applications like the spin momentum relaxation time. We also note that the pure spin transport is fundamentally different from ballistic charge transport which is dominated by a space charge field [2].

We further demonstrate that a ballistic pure spin current can generate a transverse pure charge current via an inverse spin Hall effect, and vice versa, a ballistic pure charge current can generate a transverse pure spin current via the spin Hall effect [3]. These new all optical spin Hall experiments were performed in the ballistic regime, on ultrafast time scale and nanometer spatial dimensions, and without applying any DC fields.

## References

- [1] H. Zhao *et al.*, “Temporally and spatially resolved ballistic pure spin transport”, *Phys. Rev. B* **75**, 075305 (2007).
- [2] H. Zhao *et al.*, unpublished.
- [3] H. Zhao *et al.*, “Coherence control of Hall charge and spin currents”. *Phys. Rev. Lett.* **96**, 246601 (2006).

# Single-Ion Magnetic Moments in Semiconductors

Michael E. Flatté and Jian-Ming Tang

*Department of Physics and Astronomy and Optical Science and Technology Center,  
University of Iowa, Iowa, USA, E-mail: michael\_flatte@mailaps.org*

When some magnetic ions are substituted into semiconductors they form extended spin-polarized electronic states around them. In one example, Mn substituted into GaAs, the extended spin-polarized state has a moment antiparallel to the Mn  $d$  electron spins that form the core magnetic moment of the ion. The extended states, similar to other shallow bound states in semiconductors, can overlap and merge into an impurity band at very low densities (less than 1% Mn substituted for Ga). When the extended states are spin-polarized, however, the combination of this overlap and the Pauli exclusion principle provides an energy gain if the ionic moments are oriented parallel to each other. This drives the formation of a ferromagnetic state if the magnetic ion density is sufficiently high. The large spatial size of the extended spin-polarized state also permits the magnetic properties of individual ions to be manipulated by the local environment, such as in the presence of strain or an applied electric field. This could lead to single-spin manipulation via applied electric fields, with applications to quantum computation [1,2].

The electronic structure of a single magnetic ion in a semiconductor will be described, focusing on Mn in GaAs [3]. Recent measurements via scanning tunneling microscopy (STM) that support this picture will also be described [4]. These measurements show the wave function of the extended spin-polarized state around a single magnetic ion extends over distances of several nanometers and is highly anisotropic. They also show that in the presence of strain the wave function is strongly distorted and even more anisotropic [5].

The shape of this wave function governs the magnetic interactions between neighboring moments and, hence, the stability of the ferromagnetic state. Predictions of the interaction strength between two magnetic moments, mediated by these extended spin-polarized states [3], have since been verified via STM [6]. From this a model of ferromagnetism in the insulating state of Mn-doped GaAs has been constructed.

This work was supported by ARO and ONR.

## References

- [1] D. D. Awschalom and M. E. Flatté, “Challenges for semiconductor spintronics”, *Nat. Phys.* **3**, 153 (2007).
- [2] J.-M. Tang, J. Levy, and M. E. Flatté, “All-Electrical Control of Single Ion Spins in a Semiconductor”, *Phys. Rev. Lett.* **97**, 106803 (2006).
- [3] J.-M. Tang and M. E. Flatté, “Multiband Tight-Binding Model of Local Magnetism in  $\text{Ga}_{1-x}\text{Mn}_x\text{As}$ ”, *Phys. Rev. Lett.* **92**, 047201 (2004).
- [4] A. Yakunin, *et al.*, “Spatial Structure of an Individual Mn Acceptor in GaAs”, *Phys. Rev. Lett.* **92**, 216806 (2004).
- [5] A. Yakunin, *et al.*, “Warping a single Mn acceptor wavefunction by straining the GaAs host”, *Nat. Mat.* **6**, 512-515 (2007).
- [6] D. Kitchen, *et al.*, “Atom-by-atom substitution of Mn in GaAs and visualization of their hole-mediated interactions”, *Nature* **442**, 436 (2006).

# ***Ab initio* Calculations on Complex Biomolecular Systems**

**Wai-Yim Ching**

*Department of Physics, University of Missouri-Kansas City  
E-mail: ChingW@umkc.edu*

Recent research efforts by the Electronic Structure Group (ESG) at the University of Missouri-Kansas City in the area of computational biomolecules and biomaterials will be summarized. I will present both the published and unpublished results on the electronic structure, bonding, charge distribution, mechanical and spectroscopic properties of Vitamin-B<sub>12</sub> molecules (cyanocobalamin, methyl-cobalamin, adenosylcobalamin, hydroxocobalamin), b-DNA models (with different numbers of base pairs with and without counterions), Type I Collagen model (7-2 heterotrimer model with three strands and 30 residues) and (001) surface structure of the bioceramic hydroxyapatite (Ca<sub>10</sub>(PO<sub>4</sub>)<sub>6</sub>(OH)<sub>2</sub>) crystal. The calculations were performed using first-principles density functional theory based OLCAO method. The goal is to apply the methods in condensed matter theory to complex biomolecular systems for greater insights. The importance of interdisciplinary collaborations and future direction of research along this line will be discussed.

# Impact of Neutrons on the Understanding of Dynamics in Soft-Matter and Biophysics

**Maikel C. Rheinstädter**

*Department of Physics and Astronomy, University of Missouri-Columbia, Columbia, MO  
E-mail: RheinstadterM@missouri.edu*

The spectrum of fluctuations in biomimetic and biological membranes covers a large range of time and length scales, ranging from the long wavelength undulation and bending modes of the bilayer with typical relaxation times of nanoseconds and lateral length scales of several hundred lipid molecules, down to the short-wavelength, picosecond density fluctuations involving neighboring lipid molecules. New developments and improvements in neutron scattering instruments, sample preparation and environments and, eventually, the more and more powerful neutron sources open up the possibility to study collective excitations, e.g. phonons, in artificial and biological membranes. The goal of this project is to seek relationships between collective dynamics on various length scales on the one hand, and macroscopic phenomena such as trans-membrane transport on the other hand.

The combination of various inelastic neutron scattering techniques enlarges the window of accessible momentum and energy transfers - or better: accessible length and time scales - and allows one to study structure and dynamics on length scales ranging from the nearest-neighbor distances of lipid molecules to length scales of more than 100 nm, covering time scales from about 0.1 ps to almost 1  $\mu$ s. The fluctuations are quantified by measuring the corresponding dispersion relations, i.e. the wave vector-dependence of the excitation frequencies or relaxation rates. Because biological materials lack an overall crystal structure, in order to fully characterize the fluctuations and to compare experimental results with membrane theories, the measurement must cover a very large range of length and time scales. By using multiple instruments, from spin-echo to triple-axis spectrometers, we have successfully probed these fluctuations over the desired range of length and time scales [1-5].

We present first results how bilayer permeability, elasticity and inter protein excitations can be determined from the dynamical experiments in the different regimes of length and time scales.

## References

- [1] M.C. Rheinstädter, C. Ollinger, G. Fragneto, F. Demmel and T. Salditt, Phys. Rev. Lett. **93**, 108107, 1-4 (2004).
- [2] Maikel C. Rheinstädter, Wolfgang Häußler and Tim Salditt, Phys. Rev. Lett. **97**, 048103, 1-4 (2006).
- [3] Maikel C. Rheinstädter, Tilo Seydel, Franz Demmel and Tim Salditt, Phys. Rev. E **71**, 061908, 1-8 (2005).
- [4] Maikel C. Rheinstädter, Tilo Seydel and Tim Salditt, Phys. Rev. E **75**, 011907, 1-5 (2007)
- [5] Maikel C. Rheinstädter, Tilo Seydel, Wolfgang Häußler and Tim Salditt, J. Vac. Soc. Technol. A **24**, 1191-1196 (2006).

**ABSTRACTS**  
**(POSTERS)**



# Phase Transitions in Quantum Ring and Sphere Arrays

**Kieran Mullen, Bahman Roostaei and Ethan Brown**

*Homer L. Dodge Dept. of Physics and Astronomy, The University of Oklahoma  
E-mail: kieran@ou.edu*

With the improvement in fabrication techniques on the micro- and nanometer scale, experimentalists are now able to produce atom-like electronic devices with their own unique spectra and shell structures. In particular, we may now examine periodic arrays of nanostructures without atomic analogues in which exchange-interaction, polarization, and separation may all be varied. Through the use of Monte Carlo simulation, in the classical case, and variational wave functions, in the quantum mechanical case, we search for novel properties in an array of singly-charged quantum rings and in nano-spherical shells, (sometimes called “quantum well quantum dots”). A phase transition has already been shown to exist in a similar system consisting of nanorings, making the same in nano-spherical shells seem a distinct possibility. Such control of the electron on the nano-scale may prove useful in optical and spin- or charge- based quantum information schemes.

# Effect of Magnetic Short-range Order on Spin-disorder Resistivity

A. L. Wysocki<sup>1</sup>, K. D. Belashchenko<sup>1</sup>, M. van Schilfgaarde<sup>2</sup>, J. P. Velev<sup>1</sup>

<sup>1</sup>*Department of Physics and Astronomy, University of Nebraska Lincoln*

<sup>2</sup>*Department of Chemical and Materials Engineering, Arizona State University, Tempe, Arizona*

*E-mail: awysocki@bigred.unl.edu*

In magnetic metals the resistivity has a contribution due to scattering on the thermally-induced spin fluctuations. In general, this spin-disorder resistivity (SDR) is sensitive to the magnetic short-range order (MSRO) [1]. Previously, we studied the temperature dependence of SDR for Fe and Ni using the mean-field approximation [2]. In this work we explore the effect of MSRO on SDR using the supercell technique. The disordered spin configurations are generated for a range of temperatures using Monte Carlo simulations for the classical nearest neighbor Heisenberg model. Further, different spin structures are produced using the reverse Monte Carlo method. The latter approach allows us to generate the spin configurations with predefined short-range order. The electronic structure of the system is calculated using the noncollinear version of the tight-binding linear muffin-tin method. The Kubo-Landauer approach is used to find the conductance through a slab of disordered material which is then averaged over a sufficient number of spin configurations. The calculated temperature dependence of SDR for Fe is in better agreement with experiment than in the case of mean-field approximation. These calculations indicate that the behavior of SDR in Fe is consistent with modest short-range order characteristic for the Heisenberg model. In addition, we investigate some technical aspects of SDR calculation including the importance of self-consistency and the choice of the atomic basis set.

## References

- [1] M. E. Fisher and J.S. Langer, Phys. Rev. Lett. **20**, 665 (1968).
- [2] A. L. Wysocki, K. D. Belashchenko, J. P. Velev, and M. van Schilfgaarde, J. Appl. Phys. **101**, 09G506 (2007).

# Thermodynamics of Itinerant Magnets: A Simple Classical Model with Longitudinal Spin Fluctuations

A. L. Wysocki, J. K. Glasbrenner, and K. D. Belashchenko

*Department of Physics and Astronomy, University of Nebraska - Lincoln  
E-mail: awysocki@bigred.unl.edu*

The thermodynamics of itinerant magnets is not well understood. First-principles calculations using the disordered local moment (DLM) approximation [1] fail to produce a local moment above the Curie temperature in nickel [2]. This failure is often attributed to the neglect of short-range order, which was found to be very strong in adiabatic spin-dynamics simulations [3]. However, if longitudinal spin fluctuations (LSF) are included, the local moment is recovered and the short-range order is weak [4]. The classical model used in [4] seems to be useful for itinerant magnets, but its general thermodynamic behavior has not been studied. Here we investigate it in its simplest form which contains only one “itinerancy parameter.” We performed Monte Carlo simulations and compared the results with the mean-field theory. A non-trivial complication, which has not been discussed so far, is the choice of the phase space measure for LSF. While no unique prescription within the classical model is possible, we explored two options: the “classical” measure used in [4], and the “flat” measure that removes the overweighing of large moments and better reflects the combinatorial properties of a partially filled electronic shell. Our central result is that, even in the strongly itinerant limit, the magnetic short-range order is always weak, and the mean-field theory is in very good agreement with Monte Carlo results. For the classical measure, the second-order phase transition was observed for all values of the itinerancy parameter, but for the flat measure the transition becomes first-order for even moderately itinerant systems. This feature highlights the main limitation of the model, i.e. its neglect of correct quantum atomic statistics even in the uncorrelated limit. Deviations from the Curie-Weiss law above the Curie temperature in itinerant systems are also observed and discussed.

## References

- [1] B. L. Gyorffy et. al., J. Phys. F: Met. Phys. **15**, 1337 (1985).
- [2] J. B. Staunton and B. L. Gyorffy, Phys. Rev. Lett. **69**, 371 (1992).
- [3] V. P. Antropov, Phys. Rev. B **72**, 140406(R) (2005).
- [4] N. M. Rosengaard and B. Johansson, Phys. Rev. B **55**, 14975 (1997); A. V. Ruban et. al. Phys. Rev. B **75**, 054402 (2007).

# The Origins of Tunneling Anisotropic Magnetoresistance in Nanoscale Ferromagnetic Metal Break Junctions

**J. D. Burton,<sup>1,3</sup> R. F. Sabirianov,<sup>2,3</sup> J. P. Velev,<sup>1,3</sup>, O. N. Mryasov,<sup>4</sup>  
and E. Y. Tsymbal<sup>1,3</sup>**

<sup>1</sup>*Department of Physics and Astronomy, University of Nebraska, Lincoln, Nebraska  
68588-0111, USA*

<sup>2</sup>*Department of Physics, University of Nebraska, Omaha, Nebraska 68182-0266, USA*

<sup>3</sup>*Nebraska Center for Materials and Nanoscience, University of Nebraska, Lincoln,  
Nebraska 68588-0111, USA*

<sup>4</sup>*Seagate Research, Pittsburgh, Pennsylvania 15222, USA  
E-mail: jlz101@unlserve.unl.edu*

Anisotropic magnetoresistance (AMR) is the difference in resistance as the magnetization direction is changed with respect to the direction of current flow. In bulk materials the AMR effect is small and originates from spin-orbit scattering during diffusive transport. In nano- and atomic-scale systems the effect stems directly from the variation in the electronic structure due to the spin-orbit coupling. For example, in the ballistic regime quantized steps are observed in the conductance as the magnetization angle is changed, which can be attributed to a change in number of bands crossing the Fermi energy. [1] Fully broken atomic-scale magnetic break junctions also reveal AMR in the tunneling regime [2], an effect known as tunneling AMR (TAMR). In this work we present first-principles calculations [3] of electron tunneling transport in fully broken Ni and Co break junctions which reveal strong dependence of the conductance on the magnetization direction. The origin of this phenomenon stems from resonant states localized in the electrodes near the junction break. The energy and broadening of these states is strongly affected by the magnetization orientation due to spin-orbit coupling, causing TAMR to be sensitive to bias voltage on a scale of a few mV. Our results bear a resemblance to recent experimental data [2] and suggest that TAMR driven by resonant states is a general phenomenon typical for magnetic broken contact. The same effect may be observed in any system where a magnetic tip is used to probe electronic tunneling, like in a spin-polarized scanning-tunneling geometry.

## References

- [1] J. Velev et al., Phys. Rev. Lett. 127203 (2005), A. Sokolov et al. Nature Nanotech. **2**, 171 (2007).
- [2] K. Bolotin et al., Phys. Rev. Lett. **97**, 127202 (2006).
- [3] J. D. Burton et al., cond-mat/0703345.

# Surface Induced Suppression of Magnetization in Nanoparticles

C. Westman,<sup>1</sup> S. Jang,<sup>2</sup> C. Kim,<sup>2</sup> S. He,<sup>2</sup> G. Harmon,<sup>3</sup> N. Miller,<sup>3</sup> B. Graves,<sup>3</sup> N. Poudyal,<sup>4</sup> R. Sabirianov,<sup>1</sup> H. Zeng,<sup>2</sup> M. DeMarco,<sup>2,3</sup> and J. P. Liu<sup>4</sup>

<sup>1</sup>*Department of Physics, University of Nebraska at Omaha*

<sup>2</sup>*Department of Physics, University at Buffalo, the State University of New York*

<sup>3</sup>*Department of Physics, Buffalo State College*

<sup>4</sup>*Department of Physics, University of Texas at Arlington*

*E-mail: rsabirianov@mail.unomaha.edu*

We show that the competition between FM and AFM interactions in nanoparticles can lead to surface induced suppression of the magnetization. The symmetry of surface termination of the nanoparticle may lead to a magnetic structure that is entirely non-magnetic, non-collinear or FM, depending on the relative strength of the competing exchange interactions. We consider model particles with the shape of truncated octahedron terminated by (111) and (001) facets, mimicking experimentally synthesized nanoparticles [1]. The surface ordering temperature can be lower than that of the interior of the particle, resulting in a magnetically “dead layer” at finite temperatures. This model is consistent with several of our experimental observations in FePt nanoparticles: 1. a significant paramagnetic volume fraction at finite temperatures, which is enhanced with decreasing particle size and diminished by cooling; 2. a large reduction of the zero-temperature magnetization from bulk values; 3. an unconventional temperature dependence of the magnetization which becomes more prominent in smaller sized particles.

## References

- [1] Z.R. Dai, S Sun, Z.L. Wang, Nano Lett., 1, 443 (2001); M. Chen, J. P. Liu, S. Sun, J. Am. Chem. Soc. 126, 8394 (2004).

## Surface Finite Size Effect in Nanoparticles

**J. Koch and Renat Sabirianov**

*Department of Physics, University of Nebraska, Omaha, NE 68182-0266  
E-mail: rsabirianov@mail.unomaha.edu*

The magnetic properties of single layer shell particles studied as function of the particle's size using Monte Carlo method with free boundary conditions. We formed truncated octahedron shell-nanoparticles of 12-90 lattice spacings across mimicking particles from 4-12 nm in size. The classical Heisenberg model with nearest neighbor ferromagnetic (FM) and antiferromagnetic (AFM) exchange interactions shows the existence of the well defined ground state. FM nanoparticles have susceptibility maximum decreasing with the increase of the nanoparticle size. Finite size scaling analysis predicts small Curie temperature for shells of the large size. The AFM particles built as truncated octahedron with (001) and (111) planes of the cubic lattice show freezing in the noncollinear structure with very low magnetization. The origin of noncollinearity is the frustration in the (111) plane and at the edges between (001) and (111) faces. The freezing temperature in particles with AFM does not change strongly with the size of the particle.

# Electronic Properties of LaB<sub>6</sub>: a Theoretical Study

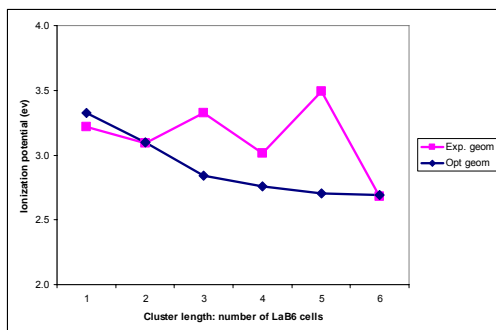
Guangping Li,<sup>1</sup> Jing Lu,<sup>1</sup> R. Sabirianov,<sup>1</sup> Wai-Ning Mei,<sup>1</sup>  
C. L. Cheung,<sup>2</sup> and X. C. Zeng<sup>2</sup>

<sup>1</sup>Department of Physics, University of Nebraska at Omaha, Omaha, Nebraska 68182,

<sup>2</sup>Department of Chemistry, University of Nebraska - Lincoln, Lincoln, Nebraska 68588

E-mail: physmei@mail.unomaha.edu

Metal hexa-borides have varieties of interesting properties and are utilized frequently in technological applications: e.g. LaB<sub>6</sub> is known to have extremely low work function (WF = 2.6 eV), thus is used as one of the most popular electron emitter. LaB<sub>6</sub> nano-rods generate stronger electric current than in the bulk case. The focus of this work is on the band structure calculations of quasi-1D nano-rods with various widths and breadths for the purpose of studying the relationship between work function and rod shape using GGA density functional theory with all electron and relativistic effect included. We use cluster model to investigate the change of ionization potential (IP) with the length of cluster (number of unit cell of LaB<sub>6</sub> in Z-direction), up to ten unit cells, and with the cross section area, i.e. 1x1x1, 2x2x1 and 3x3x1. For clusters with the cross section of one unit cell, the IP decreases with the increase of



number of unit cells, see the figure at left, from 3.3 eV for one unit cell to 2.7 eV for six unit cells, reasonably comparable to the work function of bulk LaB<sub>6</sub>. Band structure, density of state, Fermi energy, and electrostatic potential at the center of vacuum are calculated for these 1D-rods of LaB<sub>6</sub> (infinite in Z-direction). The rods have the cross section area of 1x1, 2x1, 3x1, and 2x2. The work function of

the rod is calculate as  $WF = -E(\text{electrostatic potential}) - E(\text{Fermi})$ . The measured work function of bulk LaB<sub>6</sub> changes with the sample's surface state, surface direction and amount and type of impurity on the surface. The trend is  $WF(100) < WF(110) < WF(111)$ . Therefore, various LaB<sub>6</sub> slabs are constructed to evaluate the change of work functions. In conclusion, we use both cluster and rod models to investigate the change trend of ionization potential and work function of LaB<sub>6</sub> whose nano-rods have potential for wide spread applications in electron scanning and image industry and research.

## References

- [1] Han Zhang, Jie Tang, Qi Zhang, and et al., "Field emission of electrons from single LaB<sub>6</sub> nanowires." *Advanced Materials* **18**, 87-91 (2006).
- [2] Pavel Peshev, "Lanthanum hexaborides, an 8unusual material." *Proc. 11<sup>th</sup> Int. Symp. Boron, Borides and Related Compounds*, Tsukuba, 1993. *JJAP Series* **10**, 118-123 (1994).

# **Analytical and Numerical Solution of Double Well Using Triconfluent Heun Function**

**A. Holloway, W. N. Mei, and R. F. Sabirianov**

*Department of Physics, University of Nebraska at Omaha, Omaha, NE 68182  
E-mail: aholloway@mail.unomaha.edu*

Double well potentials occur frequently in many branches of physics. Solving the Schrodinger equations involving double well potentials analytically is a difficult task, though numbers of numerical solutions are available. In this work we offer a simple and elegant solution for potential with combination of quadratic and quartic terms in the form of solutions of triconfluent Heun equation (THE). General Heun equation is a generalization of Gauss's hypergeometric equation with four versus three regular singular points; for THE, all four singular points merged in one at infinity. We obtained eigenvalues, eigenfunctions, and normalization constants for ground and excited states.

Periodic double well is suitable to model nanostructures made by ferroelectric material and produced by molecular beam epitaxy or similar techniques. Based on our knowledge, analytical and numerical solutions of the quantum-mechanical problems involving potential of this type are not available. In this work we offer for the first time an analytical method to solve periodic double well potential based on our technique similar to a single double well potential that uses solutions of THE. Consequently, we obtained eigenvalues and eigenfunctions for ground and excited states, and also their band structures.

## Mullite: Structure and Properties

Sitaram Aryal, Hongzhi Yao, and W. Y. Ching

*Department of Physics, University of Missouri-Kansas City  
E-mail: sra3zd@umkc.edu*

Mullite is an aluminosilicate represented as the solid solution series  $Al_{4+2x} Si_{2-2x} O_{10-x}$  with  $x$  varying from 0.18 to 0.88. Mullite is a disordered system with octahedral Al and tetrahedral Al and Si atoms along with oxygen vacancies in contrast to sillimanite ( $x=0$ ). It is an important structural and functional ceramic with many applications. We have constructed different supercell models of mullite for many different values of  $x$  ( $x = 0.25, 0.4, 0.67, \text{ and } 0.825$ ; aka  $3/2$  [ $3Al_2O_3 \cdot 2SiO_2$ ],  $2/1$ ,  $4/1$  and  $9/1$  mullite) from the corresponding experimental structures including the effect of partial occupation. The supercells range in size from 63 atoms up to 288 atoms. Several initial models for each  $x$  were relaxed using the Vienna Ab-initio Simulation Package (VASP) and the one with the lowest energy was taken as a representative model. Radial pair distribution functions indicate significant variations from the initial assumed structures. Electronic structure and optical properties of some of these optimized mullite models, calculated using the Density Functional Theory (DFT) based Orthogonalized Linear Combination of Atomic Orbitals (OLCAO) method, will be presented.

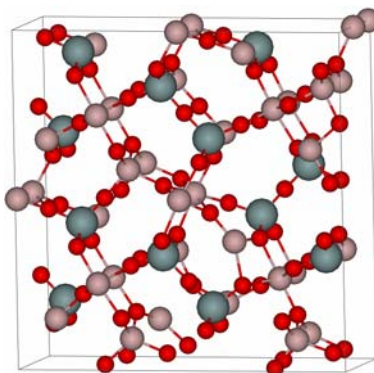


Figure1. Optimized Structure of 3/2 mullite.

# Theoretical ELNES/XANES Spectroscopic Study of a $\Sigma 5$ Grain Boundary Model in $\text{SrTiO}_3$

Paul Rulis and W. Y. Ching

*Department of Physics, University of Missouri – Kansas City*

*E-mail: rulis@umkc.edu, chingw@umkc.edu*

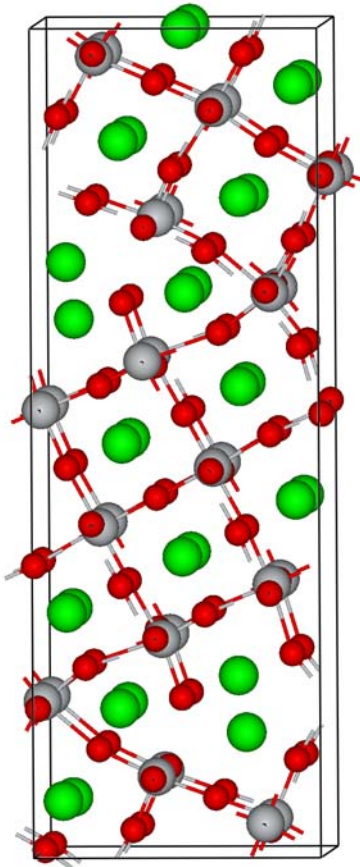


Figure 1. 140 atom  $\Sigma 5$  GB in  $\text{SrTiO}_3$ .

Microstructures and defects are an ever-present and critical fact when dealing with most solid state materials.  $\text{SrTiO}_3$  is a widely used functional material in technological applications due to its useful electronic properties, but those properties are controlled to a large extent by the presence of microstructures and defects. For example, the grain boundaries (GBs) in  $\text{SrTiO}_3$  contribute significantly to the nonlinear current-voltage characteristics of the material [1,2]. The electronic structure of the  $\Sigma 5$  GB model in  $\text{SrTiO}_3$  has been previously studied [3]. In this poster we present the results of ELNES/XANES spectral calculations of all edges of all atoms (Sr-K, Sr-L, Ti-K, Ti-L, O-K) in the model. Extensive variations of the edge structures due to local structural changes caused by the GB are vividly shown. These results can lead to the development of spectral imaging techniques for ELNES by theoretical means.

## References

- [1] N. Yamaoka, M. Masuyama, and M. Fukai, *Am. Ceram. Soc. Bull.* **62**, 698 (1983).
- [2] M. Fujimoto and W. D. Kingery, *J. Am. Ceram. Soc.* **68**, 169, (1985).
- [3] S.-D. Mo, W.-Y. Ching, M. F. Chisholm, and G. Duscher, *Phys. Rev. B* **60**, 2416 (1999).

# First-principles Investigations of the Electronic Structure and Magnetic Properties of $\text{Fe}_3\text{O}_4(001)/\text{MgO}(001)$ Interface

Hongzhi Yao<sup>1</sup>, Lizhi Ouyang<sup>2</sup> and W. Y. Ching<sup>1</sup>

<sup>1</sup>*Department of Physics, University of Missouri-Kansas City*

<sup>2</sup>*Department of Mathematics and Physics, Tennessee State University*

*E-mail: hy2mb@umkc.edu*

We carried out systematic spin-polarized density functional theory calculations on a series of low-index polar  $\text{Fe}_3\text{O}_4(001)/\text{MgO}(001)$  interfaces with possible A-terminated (occupied by tetrahedral-bonded  $\text{Fe}^{3+}$  ions) and B-terminated (occupied by octahedral-bonded  $\text{Fe}^{2+}$ ,  $\text{Fe}^{3+}$  ions and  $\text{O}^{2-}$  anions)  $\text{Fe}_3\text{O}_4(001)$  surfaces. All calculations were performed using the first principles Vienna *Ab initio* Simulation Package (VASP) with the projector-augmented wave (PAW) method and generalized gradient approximation. Our studies reveal that the model with B type of termination on  $\text{Fe}_3\text{O}_4$  with the detailed layer stacking structure as ...4Mg,4O|4Mg,4O|2Fe(B),4O|Fe(A)|2Fe(B),4O... (Fig. 1) is energetically most favorable, where (A) and (B) refer to the tetrahedral site and octahedral site respectively. Similar to bulk  $\text{Fe}_3\text{O}_4$ , the electronic structure calculations on this lowest energy model also show half-metallic properties. However, there are no enhanced magnetic moments of Fe present around the interface area. We found large polarization on O atoms at the interface with magnetic moments of about  $0.36 \mu\text{B}$ . Comparison of the same interface models with different thicknesses for the  $\text{Fe}_3\text{O}_4$  film shows the trend that thicker films result in a higher spin polarization.

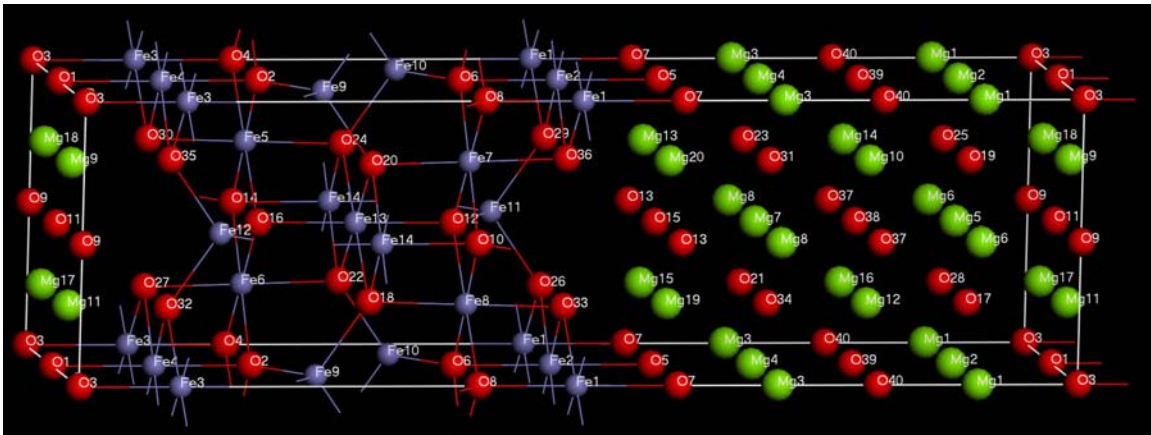
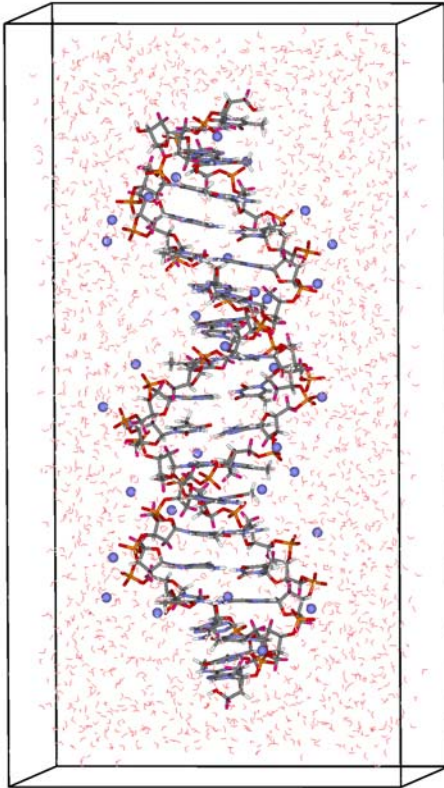


Figure 1: The  $\text{Fe}_3\text{O}_4(001)/\text{MgO}(001)$  interface model with lowest energy

## Electronic Structure of B-DNA Models

L. Liang, Paul Rulis, W.-Y. Ching

Department of Physics, University of Missouri-Kansas City  
E-Mail: ll6t6@umkc.edu, rulis@umkc.edu, ChingW@umkc.edu



DNA is a well known complex molecule with applications in the life sciences, materials sciences, and computational sciences. The properties of DNA are derived from its fundamental atomic and electronic structure for which there are few realistic large scale *ab initio* calculations. We used Amber to build two B-DNA models: One with 5 (AT) base pairs and one 17 (AT) base pairs (shown in figure 1). From the results of a 2020ps molecular dynamics Amber simulation the models were then considered in three different environments: (1) bare DNA; (2) DNA with  $\text{Na}^+$  counter ions; (3) DNA with  $\text{Na}^+$  counter ions and  $\text{H}_2\text{O}$  solvent. By using the atomic coordinates of the model, we calculated their electronic structures using the *ab initio* OLCAO method. Our preliminary studies reveal that the model's initial configuration (before the MD steps) with the addition of only  $\text{Na}^+$  ions close to the  $\text{PO}_4$  groups gives a converged potential and an insulating gap.

Figure 1. The initial configuration of B-DNA with 17(AT) base pairs,  $\text{H}_2\text{O}$  solvent, and Na counter ions.

# First-principles Calculation of MCD for Cr $L_{2,3}$ -edge XANES of $\text{CrO}_2$

Kazuyoshi Ogasawara<sup>1,2</sup>, Sachiyo Kiyozumi<sup>1</sup>

<sup>1</sup>*Department of Chemistry, Kwansei Gakuin University,  
2-1 Gakuen Sanda 669-1337 JAPAN*

<sup>2</sup>*Department of Physics, University of Missouri-Kansas City,  
5100 Rockhill Road, Kansas City, MO 64110-2499*

*E-Mail: ogasawara@ksc.kwansei.ac.jp*

Transition-metal (TM)  $L_{2,3}$ -edge X-ray absorption near-edge structure (XANES) and its magnetic circular dichroism (MCD) are effective tools for characterization of TM ions in variety of TM compounds. These spectra are generally analyzed by a modified atomic multiplet calculation approach including crystal-field effects and covalent effects as adjustable parameters. However, for the analysis of anisotropic properties in solids, an approach based on a realistic structural model is desired.

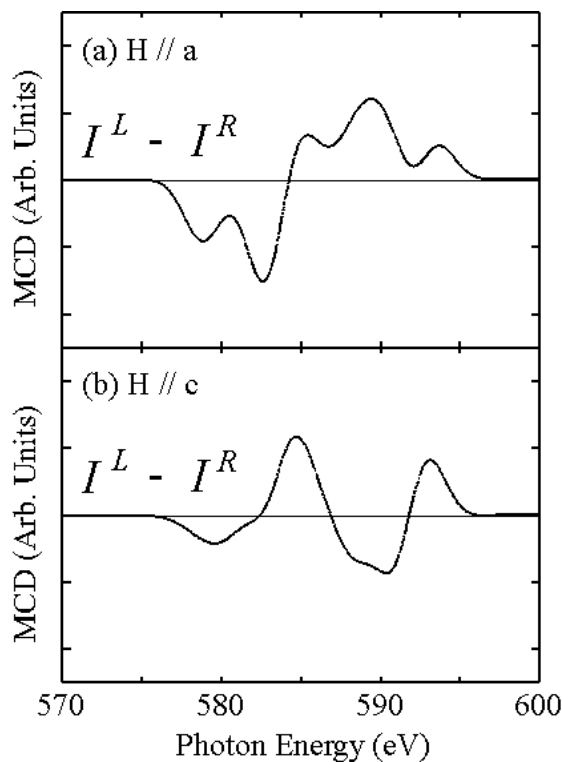


Figure 1. The theoretical MCD spectra for Cr  $L_{2,3}$ -edge XANES of  $\text{CrO}_2$  for magnetic fields parallel to (a)  $a$ -axis and (b)  $c$ -axis.

In the present work, we have performed first-principles calculation of MCD for Cr  $L_{2,3}$ -edge XANES of  $\text{CrO}_2$  using the relativistic discrete variational multielectron (DVME) code [1], which is a configuration-interaction (CI) program based on the relativistic DV- $X\alpha$  cluster method. In order to analyze the anisotropy of MCD spectra, different alignments of magnetic field were considered. The calculated MCD spectra exhibited a clear anisotropy between the spectra for the magnetic fields parallel to  $a$ -axis and  $c$ -axis, which is consistent with the experimental Cr  $L_{2,3}$ -edge MCD spectra for epitaxial  $\text{CrO}_2$  films [2].

## References

- [1] K. Ogasawara *et al.*, Phys. Rev B **64**, 115413 (2001).
- [2] E. Goering *et al.*, Phys. Rev. Lett. **88**, 207203 (2002).

## The Harris Criterion and disordered 3D Heisenberg Models

**Donald J. Priour, Jr.**

*University of Missouri, Kansas City  
E-mail: priourd@umkc.edu*

We present a direct Monte Carlo calculation testing the validity of the Harris Criterion in strongly disordered Heisenberg models (e.g., as might be used to model diluted magnetic semiconductors such as  $\text{Ga}_{1-x}\text{Mn}_x\text{As}$ ). We find self-averaging (uniformity of thermodynamic properties  $I$  in the bulk limit) to be intact. However, we find that the critical exponent  $\nu$  is altered even for very weak disorder with the shift in the universality class increasing with increasing disorder strength for both bond and site disorder. We also examine the Harris Criterion in the context of a direct antiferromagnetic superexchange coupling, finding that in this case, self averaging is violated.

# Modeling the FQHE from First Principles

**M. L. Horner and Alfred Scharff Goldhaber**

*Southern Illinois University Edwardsville, E-mail: lhorner@siue.edu*

*State University of New York Stony Brook, E-mail: goldhab@max2.physics.sunysb.edu*

Following the experimental discovery of the fractional quantum Hall effect (FQHE), Laughlin<sup>1</sup> gave an explanation and an ansatz for the many-body wave functions for the simple FQHE fractions. In a further advance Jain<sup>2,3,4</sup> introduced the 'composite fermion' [CF] description to account for general fractions.

We have a theory valid in quite a wide range, but it is tempting to ask for more: a deduction of FQHE from fundamental electromagnetic interactions. This might be one of those rare cases where rigorous deduction of the phenomena from the fundamental dynamics is within reach.

We start by discussing some very simple adiabatic processes, and with these as motivation, discuss numerical models hinting at a pathway towards deducing FQHE.

The crucial idea is that an electron in the presence of electric impurities and a strong magnetic field feels an induced magnetic field. Consider a two-dimensional Aharonov atom<sup>5</sup> in a uniform, perpendicular magnetic field. The attractive potential binding the electron to the (uncharged) 'nucleus' constrains the electron to occupy only degenerate states  $m=0$  or  $m=1$  of the lowest Landau level centered on the nucleus. For large separations of the atom and a concentrated charge, the  $m=0$  state of the atom will give the least overlap with the charge, and the lowest energy. However, at zero separation the  $m=1$  state will give the lowest energy. Because of mixing, the atom makes a transition within a diffuse ring of separation from the charge. The transition introduces an additional effective magnetic flux opposing the uniform magnetic field.

We examine results from two generations of numerical models based on these concepts. First is a one-electron model in which all but one of the electrons involved in FQHE are treated as static "impurities". This model generates half the CF downshift from applied to effective magnetic field. Second is a two-electron model testing which adds explicit anti-symmetrization of the paired state.

## References

- [1] R.B. Laughlin, "Anomalous quantum Hall effect: An incompressible quantum fluid with fractionally charged excitations", *Phys. Rev. Lett.* **50**, 1395-1398 (1983).
- [2] J.K. Jain, "Composite-fermion approach for the fractional quantum Hall effect", *Phys. Rev. Lett.* **63**, 199-202 (1989).
- [3] J.K. Jain, "Incompressible quantum Hall states", *Phys. Rev. B* **40**, 8079-8082 (1989).
- [4] J.K. Jain, "Theory of the fractional quantum Hall effect", *Phys. Rev. B* **41**, 7653-7665 (1990).
- [5] Y. Aharonov et al., "Aharonov-Bohm and Berry phases for a quantum cloud of charge", *Phys. Rev. Lett.* **73**, 918-921 (1994).

## The Electronic Band Structure of CoS<sub>2</sub>

**Ning Wu<sup>1</sup>, Ya.B. Losovyj<sup>1,2</sup>, David Wisbey<sup>1</sup>, K. Belashchenko<sup>1</sup>,  
L. Wang<sup>3</sup>, M. Manno<sup>3</sup>, C. Leighton<sup>3</sup>, and P.A. Dowben<sup>1</sup>**

<sup>1</sup>*Dept. of Physics and Astronomy and the Center for Materials Research and Analysis,  
University of Nebraska-Lincoln, Lincoln, NE 68588-0111*

<sup>2</sup>*Center for Advanced Microstructures and Devices, Louisiana State University, 6980  
Jefferson Highway, Baton Rouge, LA 70806*

<sup>3</sup>*Department of Chemical Engineering and Materials Science,  
University of Minnesota  
E-mail: ningwu@bigred.unl.edu*

Angle-resolved and energy-dependent photoemission was used to study the band structure of paramagnetic CoS<sub>2</sub> from a high-quality single-crystal samples. A strongly dispersing hybridized Co–S band is identified along the  $\Gamma$ -X line. Fermi level crossings are also analyzed along this line, and the results are interpreted using band structure calculations. The Fermi level crossings are very sensitive to the separation in the S–S dimer, and it is suggested that the half-metallic gap in CoS<sub>2</sub> may be controlled by the bonding-antibonding splitting in this dimer, rather than by exchange splitting on the Co atoms. The effective Debye temperatures of the highly spin-polarized material CoS<sub>2</sub> were measured using temperature dependent low energy electron diffraction and shown to be dependent upon electron kinetic energy. The normal dynamic motion of the (100) surface results in the effective surface Debye temperature of 326 $\pm$ 9K compared to a bulk Debye temperature of 612 $\pm$ 24K.

# Proteresis in Co:CoO Core-Shell Nanoclusters

X.-H. Wei, R. Skomski, Z.-G. Sun, and D. J. Sellmyer

*Department of Physics and Astronomy and Nebraska Center for Materials and Nanoscience, University of Nebraska, Lincoln, NE 68588*  
*E-mail: xiaohui@bigred.unl.edu*

The magnetism of ultrasmall Co:CoO core-shell nanoclusters is investigated. The structures, produced by cluster-beam deposition, have Co core sizes ranging from 1 to 7 nm and a CoO shell thickness of about 3 nm. Hysteresis loops as well as zero-field cooled and field-cooled magnetization curves have been measured and a striking feature of the nanostructures is the existence of proteretic (clockwise) rather than hysteretic loops in the core-size range from 3 to 4 nm. The proteretic behavior and its particle-size dependence reflect a subtle interplay between various anisotropies and exchange interactions in the Co and CoO phases and at the Co-CoO interface.

This research is supported by NSF-MRSEC, ONR, and NCMN.

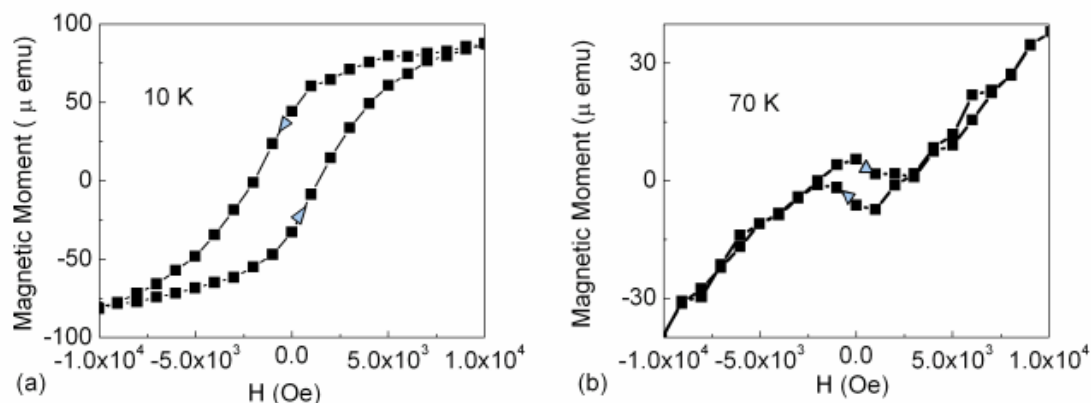


Figure. Magnetization curves for (a)  $D = 1$  nm (hysteresis) and (b)  $D = 3$  nm (proteresis).

## References

- [1] A. N. Dobrynin, D. N. Ievlev, C. Hendrich, K. Temst, P. Lievens, U. Hörmann, J. Verbeeck, G. Van Tendeloo, and A. Vantomme, *Phys. Rev. B* **73**, 245416 (2006).
- [2] M. J. O'Shea and A. L. Al-Sharif, *J. Appl. Phys.* **75**, 6673 (1994).
- [3] J. Antony, Y. Qiang, D. R. Baer, and Ch. Wang, *J. Nanosci. Nanotechnol.* **6**, 568 (2006).

# Magnetization Precession and Damping in Ni/Pt Bilayers

Steven Michalski and Roger Kirby

*Department of Physics and Astronomy and Nebraska Center for Materials and Nanoscience, University of Nebraska, Lincoln NE 68588-0111*  
*E-mail: michalsk@unlserve.unl.edu*

The study of fundamental dynamical processes such as magnetization precession and precessional damping provides insights into the behavior of complex magnetic systems, and indeed, may lead to a better understanding of the magnetization reversal process. A clear understanding of these limiting behaviors is essential if we are to overcome the technological challenges of increasing the speed and capacity of magnetic hard disk drives. In this work, the magnetization dynamics of Ni/Pt bilayers were measured using a femtosecond laser in a pump-probe experiment with direct optical excitation. This work focuses on the dependencies of the precession frequency and Gilbert damping parameter ( $\alpha$ ) on the thickness of the Ni layer and fluence of the incident pump pulse. Our measurements show that the precession frequency is independent of both the Ni layer thickness and the pump fluence, to within experimental error. Our results show that  $\alpha$  is also independent of the pump fluence, but that it increases as the Ni layer thickness decreases. Figure 1 shows the Gilbert damping parameter as a function of the Ni layer thickness for several different pump fluences. The general behavior of the average  $\alpha$  to increase with decreasing Ni thickness was expected and is similar to other reports using FMR of an increase in  $\alpha$  for very thin magnetic films surrounded by non-magnetic layers [1-3]. Tserkovnyak *et al.* in ref [4] attributed this increase in  $\alpha$  to spin pumping. Magnetization precession transfers angular momentum into the non-magnetic layer by behaving like a spin current source. This angular momentum transfer acts as an additional damping source, increasing the overall damping.

This damping is more significant for a thin sample than for a thick sample. This work is supported by NSF-MRSEC, NCMN, and the W. M. Keck Foundation.

## References

- [1] S. Mizukami, Y. Ando, and T. Miyazaki, *Phys. Rev. B* **66**, 104413 (2002).
- [2] W. B. Heinrich, Y. Tserkovnyak, G. Woltersdorf, R. Urban, and G. Bauer, *Phys. Rev. Lett.* **90**, 187601 (2003)
- [3] J. Foros, G. Woltersdorf, B. Heinrich, and A. Bratas, *J. Appl. Phys.* **97**, 10A714 (2005).
- [4] Y. Tserkovnyak, A. Bratas, and G. Bauer, *Phys. Rev. Lett.* **88**, 117601 (2002).

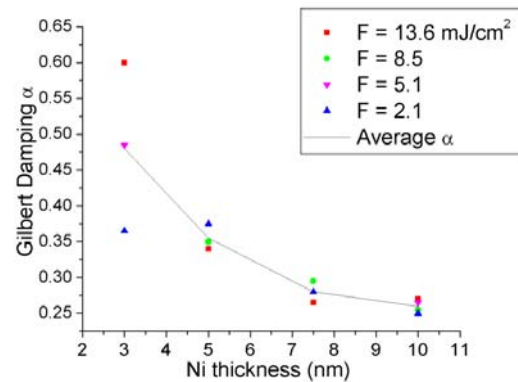


Figure 1. The Gilbert damping parameter  $\alpha$  for different Ni layer thicknesses and different fluences. The solid line represents the average  $\alpha$  for each of the Ni layers

## **L1<sub>0</sub> FePt:X Films**

**Tom A. George, Zhen Li, Minglang Yan, Yingfan Xu,  
Ralph Skomski, and David J. Sellmyer**

*Nebraska Center for Materials and Nanoscience and Department of Physics and  
Astronomy, University of Nebraska, Lincoln, NE 68588, USA  
E-mail: tageorge@bigred.unl.edu*

Non-epitaxial FePt:X films (X = Cu, Au, CuAu) with tunable magnetic properties are fabricated and investigated. Emphasis is on controlling and adjusting the magnetic properties for high-density perpendicular recording media through exchange decoupling and anisotropy. The films are initially deposited as multilayers with the structure [FePt/X]<sub>n</sub> and have individual thicknesses from about 0.06 nm to 1.1 nm. To create an (001)-oriented granular L1<sub>0</sub> structure, the films are then annealed at temperatures of 600°C for 5 minutes and 550°C for 10 minutes. The data indicate that Cu enters the L1<sub>0</sub> lattice whereas Au segregates at the grain boundaries and reduces the intergranular exchange coupling. For X = CuAu, we obtain coercivities  $H_c$  below 10 kOe, and slopes  $\alpha = (dM/dH)_{H_c}$  of about 1. For X = Cu, we find a favorable reduction in Curie-temperature and  $H_c$ . This research is supported by NSF-MRSEC, INSIC, and NCMN.

## Texture Development and Magnetic Properties of Ru-doped FePt Films

**Zhen Li, Yucheng Sui, Lanping Yue, Roger D. Kirby, David J. Sellmyer**

*Department of Physics and Astronomy and Nebraska Center for Materials and  
Nanoscience,*

*University of Nebraska, Lincoln, NE 68588-0111*

*E-mail: zhenli@bigred.unl.edu*

L1<sub>0</sub> ordered FePt films are promising candidates for ultra-high density recording media due to their high magneto-crystalline anisotropy when grown with (001) texture [1], [2]. In this work, Ru-doped FePt films are fabricated by magnetron sputtering on SiO<sub>2</sub> substrates, with subsequent annealing at 600°C for 30 minutes in forming gas (a mixture of up to 10% hydrogen in nitrogen) or pure hydrogen atmosphere. In order to understand the effects of Ru doping on the FePt L1<sub>0</sub> phase formation, we studied two different structures: (i) [Fe/Ru/Pt]<sub>n</sub> (ii) [Pt/Ru/Fe]<sub>n</sub>. For (i), with small amount Ru alloying (less than 5 at.%), (001) texture and perpendicular anisotropy remain the same. Increasing Ru concentration results in an increasing (111) texture and a steady decrease of both coercivity (H<sub>c</sub>) and saturation magnetization (M<sub>s</sub>). X-ray diffraction shows that the (001) and (002) peaks shift slightly to larger angles, indicating that Ru is dissolved into the FePt lattices. It appears that hydrogen annealing leads to improved (001) texture and larger grain size than forming gas annealing. Hydrogen atoms may occupy the interstitial sites of FePt, introducing a local strain to accelerate the diffusion and the ordering of FePt. Magnetic measurements also show higher coercivity (7.7 kOe) after hydrogen annealing, relative to 6.7 kOe after forming gas annealing. For (ii), the samples only show (111) texture independent of the amount of Ru doping. However, (001) texture could be recovered by adding a 0.5nm-thick Pt cap layer. The coercivity thus obtained is 7.2 kOe, which is much larger than that of the samples without a Pt cap layer (H<sub>c</sub>=3.5 kOe). The dramatic increase in coercivity can be attributed to the promotion of disorder/order phase transformation of the L1<sub>0</sub> FePt. For thicker Pt cap layer (2nm), the samples possess both (001) and (111) texture. Increasing thickness of the Pt cap layer lowers the degree of order and consequently reduces the (001) texture and the coercivity. —This research is supported by INSIC, NSF-MRSEC, NCMN and W.M. Keck Foundation.

### References

- [1] B. M. Lairson and M. M. Clemens, *Appl. Phys. Lett.* **63**, 1438 (1993).  
 [2] M.L.Yan, N. Powers, and D. J. Sellmyer, *J. Appl. Phys.* **93**, 8292 (2003).

# Scaling Behavior of the Exchange Bias Training Effect

Srinivas Polisetty, Sarbeswar Sahoo, and Christian Binek\*

*Department of Physics and Astronomy and the Nebraska Center for Materials and Nanoscience, University of Nebraska-Lincoln, NE 68588-0111, USA*

*\*E-mail: cbinek2@unl.edu*

Exchange-Bias (EB) is a magnetic interface effect which a ferromagnetic (FM) thin film can experience in the proximity of an antiferromagnetic (AF) pinning layer. Field-cooling of an AF/FM heterostructure to below the Néel temperature,  $T_N$ , of the AF film induces a unidirectional anisotropy revealing its presence by a shift of the FM hysteresis along the magnetic field axis called EB field. The latter degrades on subsequent cycling the FM hysteresis loops. This aging phenomenon is called training effect. Here, its dependence on temperature,  $T$ , and FM film thickness,  $t_{FM}$ , is studied in detail and scaling behavior of the data is presented. Thickness dependent EB and its training are measured using the magneto-optical Kerr effect [1]. A focused laser beam is scanned across a FM Co wedge probing hysteresis loops of the Co film. The latter is pinned by an AF CoO layer of uniform thickness. The implicit sequence

$$\mu_0 (H_{EB}(n+1) - H_{EB}(n)) = -\gamma (\mu_0 (H_{EB}(n) - H_{EB}^e))^3$$

derived from a phenomenological Landau-Khalatnikov approach is best fitted to the EB training data. They resemble the evolution of the EB field,  $H_{EB}$ , on subsequently cycled hysteresis loops,  $n$  [2,3]. The fitting parameter  $\mu_0 H_{EB}^e$  describes  $\mu_0 H_{EB}$  vs.  $n$  in the limit  $n \rightarrow \infty$  while  $\gamma$  is related to the characteristic decay rate of the training behavior. Best fits are done for various temperatures and Co thicknesses. Data collapse on respective master curves is achieved for the thickness and temperature dependent fitting parameters as well as the EB and coercive fields of the initial hysteresis loops. The scaling behavior is strong evidence for the validity and the universality of the underlying theoretical approach based on triggered relaxation of the pinning layer towards quasi-equilibrium.

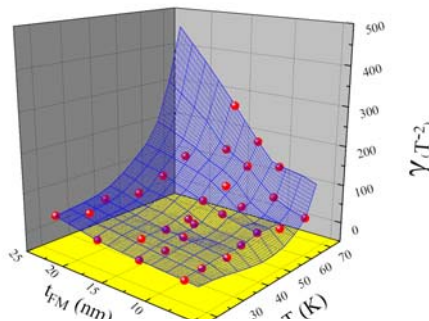


Fig. 3D plot of  $\gamma$  vs.  $(t_{FM}, T)$ .

This work is supported by NSF through Career DMR-0547887 and the MRSEC Program (DMR-0213808), and NRI.

## References

- [1] S. Polisetty, J. Scheffler, S. Sahoo, and Ch. Binek (Rev. Sc. Instr., in preparation).
- [2] Ch. Binek, Phys. Rev. B **70**, 014421 (2004).
- [3] Ch. Binek, X. He, and S. Polisetty, Phys. Rev. B **72**, 054408 (2005).

## Method to Create Cubic FePt Clusters During *in situ* Gas-Phase Aggregation

M. M. Patterson<sup>\*</sup>, X. Rui<sup>†</sup>, J. Shield<sup>†</sup> and D. J. Sellmyer<sup>†</sup>

<sup>\*</sup>University of Wisconsin – Platteville

E-mail: patterma@uwplatt.edu

<sup>†</sup>University of Nebraska at Lincoln

E-mail: dsellmyer1@unl.edu

Nanomagnetic cluster materials have wide applications as high-density storage media precursors [1]. Factors of ten increase in storage density are expected with the use of nanomagnetic clusters over present hard disc drive materials. Several methods to create nanomagnetic clusters exist, among them gas-phase aggregation in a sputter discharge. This method offers promise of a high degree of cluster property control.

The nanomagnetic FePt clusters created in the gas phase normally develop a random fcc crystal structure. The ordered phase, however, is necessary to achieve magnetic coercivities commensurate with the memory industry's future. Typically, a post-processing anneal is needed to achieve this ordered phase. However, it has been shown that *in situ* anneal is possible [2]. The method used in [2] to produce the cubic, ordered clusters is not well documented, however. Here, we present a method to create these cubic, ordered nanomagnetic FePt clusters *in situ* and propose a mechanism for the success of the method.

There are two possible reasons why clusters may form cubes. (1) The plasma conditions offer long residence times and high ion-cluster collision probability. (2) Increased current to the target heats the target atoms before they form clusters. It is also possible that (3) both effects occur synergistically.

In this study, cubic and spherical FePt clusters were created in an argon-helium dc sputter discharge under different flow and target power conditions. The plasma recipes for spherical and cubic clusters called for high He:Ar ratio, low target power and low He:Ar ratio, high target power, respectively. As measured by Langmuir probe and as expected, the recipes led to larger ion density for the cubic case ( $2 \times 10^8 \text{ cm}^{-3}$  versus  $6 \times 10^6 \text{ cm}^{-3}$  for spherical). We conclude that the larger density of argon ions increased the cluster-ion collision probability, heating the clusters *in situ* to their anneal temperature, primarily according to mechanism (2) above. This research is supported by NSF-MRSEC and NCMN.

### References

- [1] Y.F. Xu, M.L. Yan, and D.J. Sellmyer, "FePt Nanocluster Films for High-Density Magnetic Recording," Review Article, *J. Nanosci. Nanotech.* **7**, 206-224 (2007).
- [2] J-M Qiu, J-P Wang, "Monodispersed and highly ordered  $L1_0$  FePt nanoparticles prepared in the gas phase", *Appl. Phys. Lett.* **88**, 192505: 1-3 (2006).

## Photoconductive Circuit for the Study of Magnetization Precession

Robert Mumgaard, Bob Buckley, Steven Michalski and Roger Kirby

*Department of Physics and Astronomy and the Nebraska Center for Materials and Nanoscience, University of Nebraska, Lincoln*  
*E-mail: bobmumgaard@yahoo.com*

One limitation in the development of faster magnetic hard disks is the understanding of magnetic precessional dynamics in thin films. When the magnetic moment of a thin film is disturbed it precesses back to its equilibrium orientation. The study of this precession is accomplished using a femtosecond laser in a pump-probe experiment with a variable time delay between pump and pulse. Typically the pump beam launches the precession using direct optical excitation as originally shown by Ju *et al.* [1]. However, this technique requires precise alignment and introduces adverse effects due to heating of the sample. A second technique to initiate precession is to use a photoconductive circuit to create a short

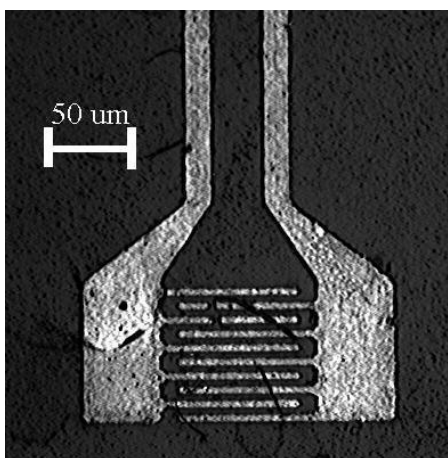


Figure 1: Optically activated portion of circuit.

magnetic field pulse. The pump beam incident on the switch causes current to flow through the circuit, creating a magnetic perturbation in the sample mounted on a circuit wire, as originally shown by Freeman *et al.* [2].

Integral to this experiment is designing a fast circuit (sub nanosecond) with small dimensions (micron). Photolithography and sputtering techniques were used to deposit several circuit designs on GaAs. These circuits were used in the pump probe experiment and their performance was examined. The initial results verify the premise of circuit launched precession. The circuits respond to the pump beam with a rise time between 50 and 100 picoseconds. However, the current circuits are time-consuming to manufacture and extremely fragile.

Current research is directed toward improving durability, current capacity and circuit response time. Streamlining the manufacture of these circuits and the evaporation deposition of a protective dielectric overcoat is planned. This work is supported by NSF-MRSEC, NCMN, and the W. M. Keck Foundation.

### References

- [1] G. Ju, A.V. Nurmikko, R. F. C. Farrow, R. F. Marks, M. J. Carey, and B. A. Gurney, *Phys. Rev. Lett.* **82**, 3705 (1999).
- [2] A. Y. Elazzabi and M. R. Freeman, *Appl. Phys. Lett.* **68**, 3456 (1996).

# Generalized Magneto-optic Ellipsometry on $\text{Zn}_{1-x}\text{Mn}_x\text{Se}$ : Dielectric and Magnetic Induced Optical Anisotropy

M. Saenger<sup>1</sup>, B. Daniel<sup>2</sup>, M. Hetterich<sup>1</sup>, T. Hofmann<sup>1</sup>, and M. Schubert<sup>1</sup>

<sup>1</sup> Department of Electrical Engineering and Nebraska Center for Materials and Nanoscience, University of Nebraska-Lincoln, USA

<sup>2</sup> Institute for Applied Physics, Universität Karlsruhe, Germany  
E-mail: saenger@engr.unl.edu

Among the dilute magnetic semiconductors the ternary alloy  $\text{Zn}_{1-x}\text{Mn}_x\text{Se}$  has originated a great interest due to its potential application as a transport or spin aligner material in spintronic devices. Magneto-optic investigations provide very useful insights into spin-dependent electronic band structure, absorption, dielectric and magnetic polarizabilities. Spectroscopic magneto-optic studies of  $\text{ZnMnSe}$  have not been exhaustive [1, 2]. Here we employ for the first time magneto-optic generalized ellipsometry at room temperature on a set of MBE grown  $\text{Zn}_{1-x}\text{Mn}_x\text{Se}$  samples to investigate the optical anisotropy due to structure phase transformation and the magnetic field induced anisotropy, both in dependence of the Mn concentration. We present a dielectric function tensor model expanded from our previous work [3], which accounts for the dielectric and for the magnetic field induced chiral anisotropy at room temperature. By virtue of this model, the  $sp-d$  exchange splitting energy in the vicinity of the bandgap transition of the  $\Gamma$ -point is identified means the magneto-optic induced birefringence, and the energy shift of the bandgap caused by the formation of wurtzite domains can be measured in dependence of the Mn concentration. Research funded by NSF in MRSEC QSPIN at the University of Nebraska-Lincoln.

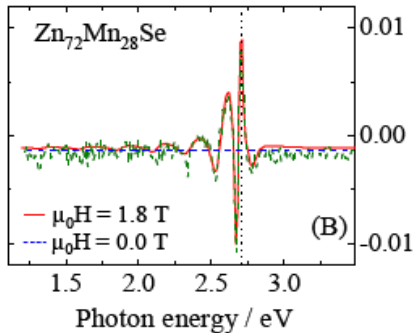


Figure 1. Experimental (green dotted line) and calculated (red solid line) Mueller matrix element  $MM_{23}$  of  $\text{Zn}_{72}\text{Mn}_{28}\text{Se}$  measured at an angle of incidence of  $2.5^\circ$  with (red line) and without (blue line) applied magnetic field. The vertical dotted line shows the position of the bandgap energy ( $E_g = 2.71$  eV).

## References

- [1] Y.X. Zheng *et al.*, Appl. Phys. **81**, 5154 (1997).
- [2] T. Yasuhira *et al.*, J. Phys. Condens. Matter **10**, 11611 (1998).
- [3] J. Kvietkova *et al.*, Phys. Rev. B **70**, 045316 (2004).

## Magnetocaloric Properties of Co/Cr Multilayers

**T. Mukherjee, S. Sahoo, R. Skomski, D. J. Sellmyer, and Ch. Binek**

*Department of Physics & Astronomy and the Nebraska Center for Materials and Nanoscience, University of Nebraska-Lincoln, Lincoln, NE, 68588-0111  
E-mail: cbinek2@unl.edu*

Current research activities in magnetocaloric materials science focus to a large extent on Gd based bulk alloys. This traditional approach has its limitations in the flexibility of tailoring microscopic parameters which in turn determine the macroscopic magnetic properties. However, controlled growth of ultra thin films allows new ways of tailoring various magnetic properties. For instance, the interlayer exchange coupling between ferromagnetic (FM) films can be tailored through variation of the thickness of nonmagnetic spacer layers. Our approach uses multilayer structures of exchange interacting thin films to tailor properties such as intra- and interlayer exchange in a wide parameter space [1]. We focus on the realization of a strong temperature dependence of the magnetization which is a key element for materials in high-efficiency magnetocaloric cooling applications. For instance, the critical temperature of FM Co layers is shifted from its bulk value of 1388K down to room temperature. In addition interlayer coupling between ultra-thin Co layers is tailored in Co/Cr multilayer structures. Special emphasis is laid on Co/Cr superlattices with antiferromagnetic interlayer coupling because large magnetic entropy changes have been reported recently for bulk materials undergoing a field-induced metamagnetic transition. Moreover, Cr is an itinerant antiferromagnet with bulk Néel temperatures of 311K which is again close to room temperature where we intend to maximize the magnetic entropy changes of our samples. Our superlattices are grown by Molecular Beam Epitaxy on (111) oriented Al<sub>2</sub>O<sub>3</sub> substrates at a base pressure of  $1 \times 10^{-10}$  mbar. Structural characterization involves large angle X-ray diffraction and small angle X-ray reflectivity. The magnetic and magnetocaloric properties of the multilayers are investigated using SQUID magnetometry. The entropy changes are calculated with the help of Maxwell's relation using isothermal magnetization data sets for various applied magnetic fields below 1T.

### **Acknowledgement:**

Financial support by Nebraska Center for Energy Sciences Research (NCESR) is gratefully acknowledged.

### **References**

- [1] R. Skomski, Ch. Binek, T. Mukherjee, S. Sahoo, and D. J. Sellmyer, J. Appl. Phys., submitted (2007).

## Advanced MFM Probes for Magnetic Domain Imaging of both Hard and Soft Magnetic Films

L. Nicholl<sup>1</sup>, R. Zhang<sup>1</sup>, S. H. Liou<sup>1</sup>, L. Yuan<sup>2</sup>, D. Pappas<sup>2</sup>,  
and Bao Shan Han<sup>3</sup>

1) Department of Physics and Astronomy and Nebraska Center for Materials and Nanoscience, University of Nebraska, Lincoln, NE 68588-0111, USA

2) Quantum Device Group, 325 Broadway, National Institute of Standard and Technology, Boulder, CO 80305, USA.

3) State Key Laboratory of Magnetism, Institute of Physics, Chinese Academy of Sciences, Beijing 100080 China.

E-mail: lnicholl@unlserve.unl.edu

Selecting an appropriate probe for the sample type is important when imaging magnetic domains using magnetic force microscopy (MFM). If the stray field of the sample approaches the coercivity of the tip, the magnetization direction of the tip can change during imaging, producing a noticeable change in the brightness levels of the image. If the coercivity of the sample is smaller than the stray field of the tip, the domain structure of the sample can be altered. We have fabricated advanced probes with  $L1_0$  phase FePt that can image the domain structure of both hard and soft magnetic materials. We deposited 5 nm to 30 nm of FePt onto commercially available Si tips. After annealing at 650 °C for 1-2 hours to obtain the  $L1_0$  phase, the probes were magnetized in a 7 T field along a direction  $10^\circ$  from the z-axis, producing tips with a magnetization direction perpendicular to the sample surface. These tips were used to image the domain structure of a permanent magnet as shown in figure 1. Since the domain pattern does not reverse its brightness levels partway through the image, this shows we have produced tips with coercivities high enough for imaging the domain structure of permanent magnets. We used the same tips to image the vortex state in the center of Permalloy dots. Since the vortex is easy to move, imaging dots with an unperturbed vortex in the center shows that the stray field strength of our tip must be smaller than the coercivity of the sample, even at lift heights between 5 nm and 20 nm—which are necessary for high resolution imaging. These results show that our probes have the high coercivity and low stray field necessary for imaging both hard and soft magnetic materials.

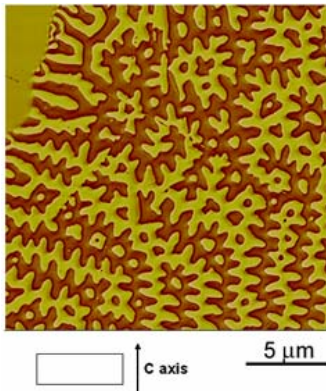


Figure 1: Permanent magnet imaged with our advanced tips. The surface normal is parallel to the  $c$  axis.

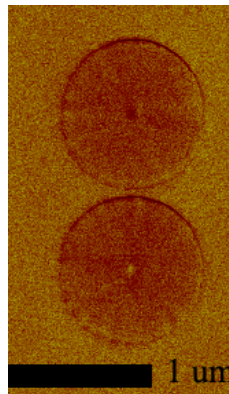


Figure 2: Domain images of permalloy dots. The easily displaced vortex center is clearly visible in the center of the dots.

# Study of Noise in Magnetic Tunneling Junction Sensors with a 64-elements Symmetric Bridge

R. Zhang<sup>1</sup>, S. H. Liou<sup>1</sup>, Stephen E. Russek,<sup>2</sup> L. Yuan,<sup>2</sup> S. T. Halloran,<sup>2</sup>  
and D. P. Pappas<sup>2</sup>

*1. Department of Physics and Astronomy and Nebraska Center for Materials and Nanoscience, University of Nebraska-Lincoln, Lincoln, NE 68588-0111, USA*

*2. National Institute of Standards and Technology, Boulder, CO 80305*

*E-mail: ruizhang@bigred.unl.edu*

The minimum detectable field of magnetoresistive sensors is limited by their intrinsic noise. Magnetization fluctuations are one of the crucial noise sources and are related to the magnetization alignment at the antiferromagnetic (AFM) – ferromagnetic (FM) interface. It is very sensitive to the dynamics and disorder in the magnetic system.

The magnetic tunnel junctions (MTJ) structure used in this study is as follows: 5 nm Ta / 5 nm Cu / 10 nm Ir<sub>20</sub>Mn<sub>80</sub> / 2 nm Co<sub>90</sub>Fe<sub>10</sub> / 0.85 nm Ru / 3 nm Co<sub>60</sub>Fe<sub>20</sub>B<sub>20</sub> / 1.4 nm Al<sub>2</sub>O<sub>3</sub> / 2 nm Co<sub>90</sub>Fe<sub>10</sub> / 28 nm Ni<sub>80</sub>Fe<sub>20</sub> / 5 nm Ta / 5 nm Ru. The junctions were patterned into 5 μm x 7.5 μm or 10 μm x 15 μm ellipses and were configured into 64-element symmetric bridges. We then investigated the low frequency noise of MTJs annealed in the temperature range from 265 °C to 305 °C with external magnetic fields applied up to 7 Tesla, in either helium or hydrogen environments. Annealing aims at improving the degree of the magnetization alignment at the AFM – FM interface as well as the quality of FM and AFM layers.

Our results indicate that the magnetic fluctuators in these MTJs changed their frequency based on annealing field and temperature. The noise of the MTJs at low frequency can be reduced by annealing under high magnetic field (7 T) and further improved by annealing in a hydrogen environment. [1]

## References

[1] S.H. Liou, R.Zhang, Stephen E. Russek, L.Yuan, S. T. Halloran, and D. P. Pappas, in press.

# **Magneto-Electric Coupling in Ferromagnetic Cobalt/Ferroelectric Copolymer Multi-Layer Films**

**A. Mardana, M. Bai\*, A. Baruth, T. Reece, S. Ducharme, S. Adenwalla**

*Department of Physics and Astronomy & Nebraska Center for Materials and Nanoscience, University of Nebraska-Lincoln,  
\*University of Missouri-Columbia  
E-Mail: abhijit@bigred.unl.edu*

The development of magnetoelectric materials that can respond to magnetic (electric) fields by changing their electrical polarization (magnetization) is of great interest. An investigation of the interactions in thin film heterostructures of metallic ferromagnets and polymer ferroelectrics has been undertaken. The samples consist of Platinum (10nm seed layer)/ ferromagnetic Cobalt (10 nm)/ferroelectric polymer (PVDF-TrFE)/ ferromagnetic Cobalt (10 nm)/ Pt (5nm cap layer). Thin Al (2nm) layers are evaporated on either side of polymer to prevent the diffusion of cobalt into the polymer. The ferroelectric polymer films of varying thickness are deposited by the Langmuir-Blodgett technique. The ferromagnetic and ferroelectric layers of the samples have been characterized by the Magneto-Optical Kerr Effect (MOKE) and the pyroelectric effect, respectively. Measurements of the electrical polarization vs. magnetic field, of magnetization changes with electrical polarization and tunneling measurements across the PVDF tunnel junction will be shown.

NSF Grant No MRSEC DMR-0213808

# Electroresistance in Ferroelectric Tunnel Junctions with Asymmetric Polar Interfaces

**J. Snodgrass and R. F. Sabirianov**

*Department of Physics, University of Nebraska, Omaha, NE 68182-0266*  
*E-mail: rsabirianov@mail.unomaha.edu*

We propose a novel mechanism for the resistive switching in ferroelectric systems with polar surfaces or interfaces. This mechanism is based on the enhancement/reduction of electric polarization in thin films with asymmetric interfaces exhibiting asymmetric interface dipole layers. We applied the phenomenological theory of a ferroelectric film with polar interfaces [1]. We show that the polarization can be enhanced when polarity of the dipole layers are in the direction of polarization of the thin film and reduced otherwise. The changes abruptly the potential profile across this structure upon the reversal of polarization by external applied electric field (voltage). This provides a two-terminal electrical control of the resistance, including the possibility of controllable switching from high resistance state (HRS) to low resistance state (LRS). The conductance of the tunnel junction calculated using the Landauer formula show that electroresistive effect can be considerably larger than in systems with symmetric interfaces.

## References

- [1] M. Ye. Zhuravlev, R. F. Sabirianov, S. S. Jaswal, and E. Y. Tsymbal, Phys. Rev. Lett. **94**, 246802 (2005).

# Synthesis of the Giant Dielectric Constant Material CaCu<sub>3</sub>Ti<sub>4</sub>O<sub>12</sub> by Wet-Chemistry Methods

Jianjun Liu,<sup>1</sup> Robert W. Smith,<sup>2</sup> Wai-Ning Mei<sup>1</sup>

<sup>1</sup>Department of Physics, University of Nebraska at Omaha, Omaha, Nebraska, 68182,

<sup>2</sup>Department of Chemistry, University of Nebraska at Omaha, Omaha, Nebraska 68182,

E-mail: jianjunliu@mail.unomaha.edu

CaCu<sub>3</sub>Ti<sub>4</sub>O<sub>12</sub> (CCTO) has been extensively investigated recently because of its giant dielectric constant, with values up to 10<sup>5</sup> at room temperature [1,2]. CCTO is usually made by standard solid-state reactions from stoichiometric ratios of CaCO<sub>3</sub>, CuO, and TiO<sub>2</sub> at high temperatures, which requires repetitive grinding and firing at high temperatures and long reaction times (e.g., 1000 °C and 20 hours). In this study, we developed a wet-chemistry method to synthesize CCTO at lower temperatures and shorter reaction times than that afforded by solid-state reactions.

In a typical experiment, stoichiometric amounts of titanium(IV) isopropoxide, calcium nitrate tetrahydrate and copper nitrate hemipentahydrate were mixed with acetylacetone, citric acid, and deionized water to get a clear solution. The solution was heated to evaporate the water, resulting in a highly viscous blue gel. The gel was placed in a preheated box oven at 450 °C for 15 minutes to obtain the precursor. Then the precursor

was heat-treated at 500-800 °C for 30 minutes and 2 hours. The resultant samples were characterized by X-ray diffraction and scanning electron microscopy.

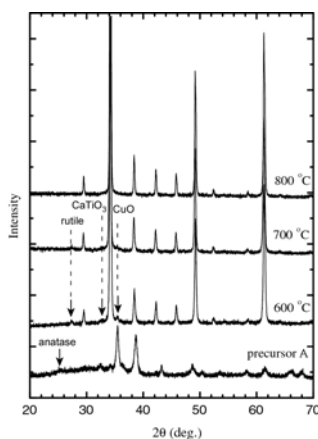


Figure 1 shows the X-ray diffractions of the precursor heat-treated at different temperature for 2 hours. At 600 °C, the precursor is converted to CCTO with small amounts of CuO, rutile (TiO<sub>2</sub>), and CaTiO<sub>3</sub>. The impurities drastically decrease at 700 °C and become undetectable at 800 °C.

Fig. 1: X-ray diffractions of the resultant products after the precursor was heat-treated for 2 hour at different temperatures.

In conclusion, we developed a new wet-chemistry method to make the giant dielectric constant material CCTO with which the pure CCTO can be synthesized at 800 °C for 2 hours.

## References

- [1] M. A. Subramanian, D. Li, N. Duan, B. A. Reisner, A. W. Sleight, *J. Solid State Chem.* **151**, 323–325 (2000).
- [2] C. C. Homes, T. Vogt, S. M. Shapiro, S. Wakimoto, A. P. Ramirez, *Science* **293**, 673–676 (2001).

# Piezomagnetic Effect in Mn-Based Antiperovskites

Pavel Lukashev<sup>1</sup> and Renat Sabirianov<sup>2</sup>

<sup>1</sup>*Department of Physics and Astronomy, University of Nebraska - Lincoln*

<sup>2</sup>*Department of Physics, University of Nebraska at Omaha*

*E-mail: rsabirianov@mail.unomaha.edu*

Recent experimental and theoretical studies of the magnetoelectric (ME) effect in the nanocomposite structures and in laminates show an enhanced ME coefficient.<sup>1</sup> These materials combine piezoelectric properties of the paramagnetic phase and piezomagnetic properties of the magnetic phase. We propose to fabricate heterostructures formed by piezoelectric materials and magnetic antiperovskites (AP) as magnetoelectric materials. We show that the magnetic structure of antiperovskite, such as  $\text{Mn}_3\text{XN}$  ( $\text{X}=\text{Ga}, \text{Zn}$ ), can be changed by a small applied biaxial strain. The lowering of symmetry with the strain causes the local magnetic moments of Mn atoms to rotate from the trigonal  $\Gamma^{5g}$  structure with symmetric curl of spin density in the (111)-plane to a monoclinic symmetry structure. As a result, an appreciable net magnetization appears in the strained system. Assuming optimistic values of parameters in two phase composite resulting in  $0.03\mu_B$  change in the magnetic moment per unit cell upon polarization, the average ME coefficient is about  $0.001 \text{ G}\cdot\text{cm}/\text{V}$ , which corresponds to  $\alpha = 1 \cdot 10^{-9} \text{ s/m}$  ( $\text{Cr}_2\text{O}_3$  has a three orders of magnitude lower value of  $\alpha = 2.67 \cdot 10^{-12} \text{ s/m}$ ). This ME coefficient is large and comparable to recently reported measurements in epitaxial  $\text{BiFeO}_3/\text{CoFe}_2\text{O}_4$  nanocomposites.<sup>1</sup>

## References

- [1] F. Zavaliche, H. Zheng, L. Mohaddes-Ardabili, S.Y. Yang, Q. Zhan, P. Shafer, E. Reilly, R. Chopdekar, Y. Jia, P. Wright, D.G. Schlom, Y. Suzuki, and R. Ramesh, *Nano Lett.* **5**, 1793 (2005).

# Electron Transport in Ferroelectric and Multiferroic Tunnel Junctions

**Julian P. Velev, Chun-Gang Duan, Kirill D. Belashchenko,  
Sitaram S. Jaswal, and Evgeny Y. Tsymbal**

*Department of Physics and Astronomy, Nebraska Center for Materials and Nanoscience,  
University of Nebraska, Lincoln, USA*

*E-mail:*

In the past decade the phenomena of electron tunneling and ferroelectricity have attracted significant interest due to their potential applications in thin-film electronic devices such as magnetic tunnel junctions and non-volatile ferroelectric memories. Recently, driven by demonstrations of ferroelectricity in ultrathin films, the idea to combine these two phenomena in a unique electronic device utilizing a ferroelectric barrier in a tunnel junction was proposed [1]. In this work we use first-principles electronic structure and transport calculations to demonstrate the impact of the electric polarization on electron transport in Pt/BaTiO<sub>3</sub>/Pt ferroelectric tunnel junctions (FTJ) and spin transport in Fe/BaTiO<sub>3</sub>/Fe multiferroic tunnel junction (MFTJ). We find that the polarization of BaTiO<sub>3</sub> reduces the tunneling conductance, as compared to a non-polarized barrier, due to the change in the electronic structure driven by ferroelectric displacements in both Pt/BaTiO<sub>3</sub>/Pt [2] and Fe/BaTiO<sub>3</sub>/Fe [3] TJs. For the MFTJ, however, this effect has different magnitude for majority- and minority-spin channels and for parallel and antiparallel orientation of the magnetization of the electrodes. As a result, we find a drop in the spin polarization of the tunneling current in the parallel configuration and an inversion of the magnetoresistance as polarization of the barrier is turned on. These results reveal exciting prospects that FTJs and MFTJs may offer as magnetoresistive switches in nanoscale spintronics devices. Supported by NSF-MRSEC.

- [1] E. Y. Tsymbal and H. Kohlstedt, *Science* **313**, 181 (2006).
- [2] J. P. Velev, C.-G. Duan, K. D. Belashchenko, S. S. Jaswal, and E. Y. Tsymbal, *Phys. Rev. Lett.* **98**, 137201 (2007).
- [3] J. P. Velev, C.-G. Duan, K. D. Belashchenko, S. S. Jaswal, and E. Y. Tsymbal, *Phys. J. Appl. Phys.* (accepted for publication).

# Ferroelectric Control of Magnetism in BaTiO<sub>3</sub>/Fe Heterostructures

Srinivas Polisetty, Sarbeswar Sahoo, Chun-Gang Duan, Sitaram S. Jaswal, Evgeny Y. Tsymbal, and Christian Binek\*

Department of Physics and Astronomy and the Nebraska Center for Materials and Nanoscience, University of Nebraska, Lincoln, Nebraska 68588-0111, USA

\*E-mail: cbinek2@unl.edu

Reversible control of magnetism is reported for a Fe thin film in proximity of a BaTiO<sub>3</sub> single-crystal. Large magnetization changes emerge in response to ferroelectric (FE) switching and structural transitions of BaTiO<sub>3</sub> controlled by applied electric fields and temperature, respectively. Interface strain coupling is the primary mechanism altering the induced magnetic anisotropy. As a result, coercivity changes up to 120% occur between the various structural states of BaTiO<sub>3</sub>. Up to 20% coercivity change is achieved via

electrical control at room temperature [1]. Our all solid state FE-ferromagnetic heterostructures open viable possibilities for new technological applications.

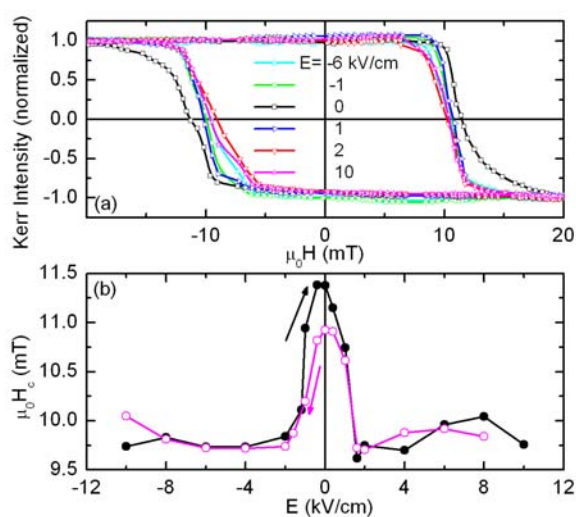


Fig.: (a) Normalized Kerr magnetic loops at room temperature measured at different applied electric fields  $-10\text{ kV/cm} < E < 10\text{ kV/cm}$ . (b)  $\mu_0 H_c$  vs.  $E$  as obtained from loops in (a). Arrows point to directions along which the change of electric fields takes place in steps.

## Acknowledgement:

This research was supported by NSF through Career DMR-0547887, MRSEC DMR-0213808, and NRI

## References

- [1] Sarbeswar Sahoo, Srinivas Polisetty, Chun-Gang Duan, Sitaram S. Jaswal, Evgeny Y. Tsymbal, and Christian Binek, Phys. Rev. B **76** (2007).

# Magnetic and Magnetoelectric Properties of Epitaxial $\text{Cr}_2\text{O}_3$ Thin Films

Xi He, Yi Wang, Sarbeswar Sahoo, and Christian Binek\*

*Department of Physics and Astronomy and the Nebraska Center for Materials and Nanoscience, University of Nebraska-Lincoln, NE 68588-0111, USA*

*\* E-mail: cbinek2@unl.edu*

Electrically controlled exchange bias (EB) is potentially useful for novel spintronic applications [1]. The basic effects of electrically controlled EB and its magnetoelectric (ME) switching are studied in  $\text{Cr}_2\text{O}_3(111)/(\text{Co}/\text{Pt})_3$  heterostructures. Here, exchange coupling between the ME antiferromagnet  $\text{Cr}_2\text{O}_3$  and a ferromagnetic (FM) CoPt multilayer gives rise to perpendicular EB. The latter is controlled by applied axial electric fields inducing excess magnetization at the interface of the antiferromagnetic (AF)  $\text{Cr}_2\text{O}_3$  pinning layer. The enhancement of this hitherto weak tuning effect is explored when replacing ME bulk pinning systems by epitaxial thin films. Therefore, growth and systematic characterization of structural, dielectric, magnetic and ME properties of epitaxial  $\text{Cr}_2\text{O}_3$  thin films is in order. We investigate the crossover from thick  $\text{Cr}_2\text{O}_3$  films with AF and ME bulk properties to the magnetic and ME behavior of  $\text{Cr}_2\text{O}_3$  thin films. Recently interesting thin film anomalies like spontaneous magnetization and shifts of the magnetic ordering temperature have been observed [2]. Here, we focus on the evolution of the ME properties with decreasing film thickness. X-Ray Diffraction (XRD) and X-Ray Reflectometry (XRR) are used to analyze the structure of  $\text{Cr}_2\text{O}_3$  epitaxial thin films. Magnetic and ME properties of  $\text{Cr}_2\text{O}_3$  films are studied via SQUID magnetometry and magneto-optical Kerr effect (MOKE), respectively.

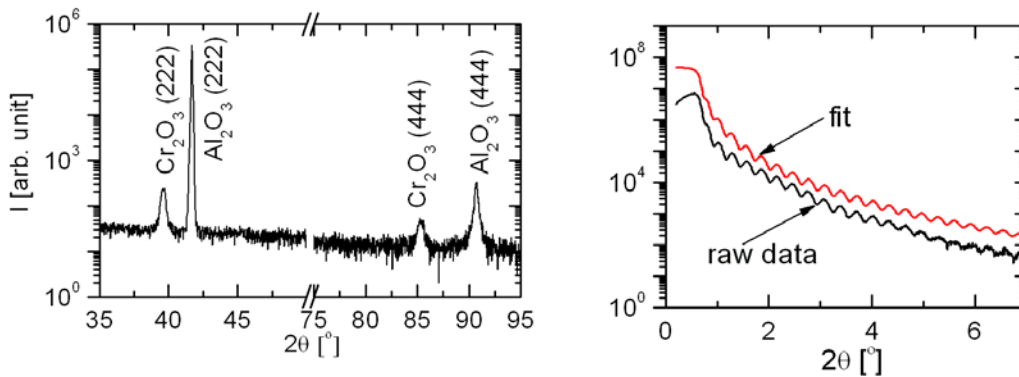


Fig.: XRD and XRR data of a 27.8 nm thick  $\text{Cr}_2\text{O}_3$  films on sapphire c-plane.

## References

- [1] Ch.Binek and B.Doudin, *J. Phys. Condens. Matter* **17**, L39 (2005).
- [2] S. Sahoo and Ch. Binek, *Phil. Mag. Lett.* **87**, 259 (2007).

## Magnetism of LaAlO<sub>3</sub>/SrTiO<sub>3</sub> Superlattices

**Karolina Janicka, Julian P. Velev and Evgeny Y. Tsybal**

*Department of Physics and Astronomy, Nebraska Center for Materials and Nanoscience,  
University of Nebraska, Lincoln, USA  
E-mail: janicka@bigred.unl.edu*

The discovery of highly conducting interface between two insulating oxides LaAlO<sub>3</sub> and SrTiO<sub>3</sub> has attracted significant interest due to possible applications in all-oxide high-electron mobility transistors [1]. Very recently, the evidence of magnetism at the interface between these non-magnetic oxides was found which may open exciting perspectives for spintronics applications [2]. Stimulated by this discovery we perform first-principles electronic structure calculations to elucidate the magnetism of LaAlO<sub>3</sub>/SrTiO<sub>3</sub> superlattices. We find that TiO<sub>2</sub>-terminated interfaces are *n*-type conducting which is consistent with experimental observations [1]. The spin-polarized calculations within the local density approximation (LDA) reveal that this interface in a (LaAlO<sub>3</sub>)<sub>3</sub>/(SrTiO<sub>3</sub>)<sub>3</sub> superlattice is magnetic with magnetic moment on the Ti<sup>3+</sup> atom of 0.2μ<sub>B</sub>. For thicker SrTiO<sub>3</sub> layers the magnetism decreases and eventually disappears because the electron gas spreads over more than one unit cell making the electron delocalized across the superlattice and violating the Stoner criterion for magnetism. Thus, the interface magnetization in these superlattices is due to geometric confinement of the electron gas. The inclusion of electron correlations via the LDA+U approximation with U=5eV on the interface Ti atom enhances the interface magnetization and makes the two-dimensional electron gas half-metallic. Supported by NSF-MRSEC.

[1] A. Ohtomo, D. A. Muller, J. L. Grazul, and H. Y. Hwang, *Nature* **419**, 378 (2002).

[2] A. Brinkman, M. Huijben, M. van Zalk, J. Huijben, U. Zeitler, J.C. Maan, W.G. van der Wiel, G. Rijnders, D.H.A. Blank, H. Hilgenkamp, *Nature Mater.*, in press (3 June 2007).

## Structure of Langmuir-Blodgett Films of Vinylidene Fluoride Oligomers

Yong Wang,<sup>1</sup> Jihee Kim,<sup>1</sup> Nick Reding,<sup>1</sup> Kristin Kraemer,<sup>1</sup> Stephen Ducharme,<sup>1</sup> Zhongxin Ge,<sup>2</sup> James M. Takacs<sup>2</sup>

<sup>1</sup>*Department of Physics and Astronomy*

<sup>2</sup>*Department of Chemistry*

*Nebraska Center for Materials and Nanoscience*

*University of Nebraska, Lincoln, NE 68588*

*E-mail: sducharme1@unl.edu*

Oligomer analogs of polyvinylidene fluoride (PVDF) with chain length much shorter than that of PVDF are an extremely interesting new ferroelectric system that can be formed by molecular self assembly. We synthesized the iodine oligomer [1] with the chemical structure  $\text{CF}_3 - (\text{CH}_2\text{CF}_2)_n - \text{I}$ . Oligomer films with  $n = 14$  were made by Langmuir-Blodgett (LB)

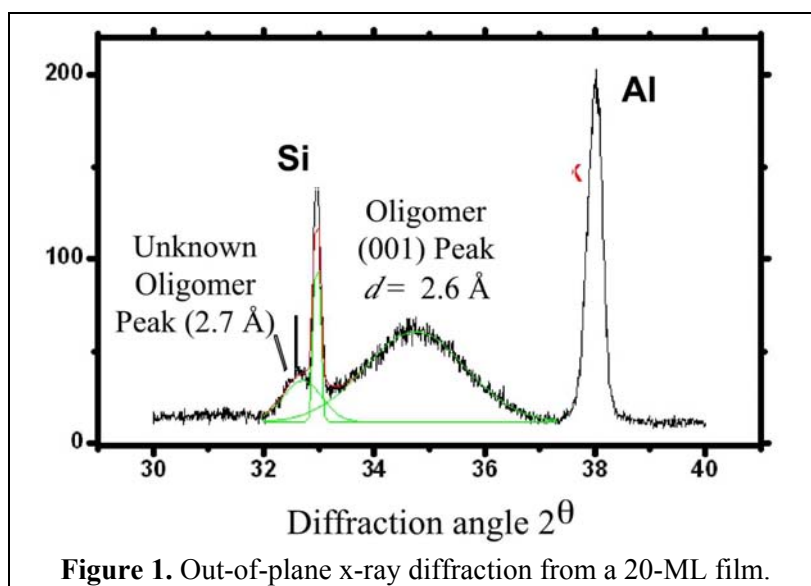


**Figure 1.** Out-of-plane x-ray diffraction from a 20-ML film.

deposition at different pressure for different layers. By using X-ray diffraction (XRD), we obtained lattice parameters for the Iodine Oligomer in the space group  $C_{222}$  after annealed at  $125\text{ C}^\circ$  and found that they form crystalline monolayers with most chains perpendicular to the film [Fig. 1]. From both temperature-dependent x-ray diffraction and the dependence of capacitance on temperature, it is conclude that there are no phase transitions from room temperature to  $130\text{ C}^\circ$  and the structure is stable in this temperature region. We also report on similar studies of the structure VDF oligomers with  $n = 10$  to  $14$ , and terminated with OH instead of Iodine.

This work was supported by the Nebraska Research Initiative.

### References

[1] K. Noda, K. Ishida, T. Horiuchi, K. Matsushige, A. Kubono, *J. Appl. Phys.* **86**, 3688 (1999).

# Modeling the Small Signal Capacitance-Voltage Characteristics of Metal-Ferroelectric-Insulator-Memory Elements Based on Langmuir-Blodgett Copolymer Films

T. J. Reece and Stephen Ducharme

*Department of Physics and Astronomy; Nebraska Center for Materials and Nanoscience  
University of Nebraska, Lincoln, NE 68588  
E-mail: sducharme1@unl.edu*

Ferroelectric memories have attracted much attention recently because of the potentially lower writing voltages and switching speeds than those of flash memory. The metal-ferroelectric-insulator-semiconductor field effect transistor (MFIS-FET) type has a number of distinct advantages, including nondestructive readout and a scalable single device structure. It has been noted that the MFIS-FET will be the mainstream of high density (tens of MBit to GBit) nonvolatile RAM in the future [1]. The characteristics of the ferroelectric copolymer polyvinylidene fluoride (PVDF) with trifluoroethylene (TrFE), such as low dielectric constant and low temperature anneal, make it ideally suited for this memory type.

A successful model developed by Miller and McWhorter [2] was used to investigate a specific MFIS structure consisting of a 20 nm thick copolymer film on p-type silicon with a high dielectric constant (25) layer hafnium oxide layer only 10 nm [3]. We show that under ideal conditions, the memory element can be saturated at 12 Volt gate operation with a large 5 Volt memory window. Depolarization fields were also calculated and shown to approach the ferroelectric coercive field  $E_C = 125$  MV/m, which may effect state retention time. Furthermore, we discuss the effect of phenomena that are not included in the model, such as charge injection and leakage.

This work was supported by the National Science Foundation.

## References

- [1] S. B. Xiong, S. Sakai, *Appl. Phys. Lett.* **75**, 1613-1615 (1999).
- [2] S. L. Miller, P.J. McWhorter, *J. Appl. Phys.* **72**, 5999-6010 (1992).
- [3] A. Gerber, M. Fitsilis, H. Kohlstedt, R. Waser, T. J. Reece, S. Ducharme, E. Rije, *J. Appl. Phys.* **100**, 5 (2006).

## Locally Probed Ferroelectricity of Ferroelectric Nanomesas by Piezoresponse Force Microscopy

Jihee Kim,<sup>1</sup> Stephen Ducharme,<sup>1</sup> Brian Rodriguez,<sup>2</sup> Stephen Jesse,<sup>2</sup>  
Sergei V. Kalinin<sup>2</sup>

<sup>1</sup>*Department of Physics and Astronomy; Nebraska Center for Materials and Nanoscience  
University of Nebraska, Lincoln, NE 68588; E-mail: sducharme1@unl.edu*

<sup>2</sup>*Materials Science and Technology Division  
Oak Ridge National Laboratory, Oak Ridge, TN 37831; E-mail: sergei2@ornl.gov*

Nanomesas are self assembled ferroelectric crystals formed from Langmuir-Blodgett (LB) films of copolymers of polyvinylidene fluoride with trifluoroethylene (P(VDF-TrFE)) through annealing. Nanomesas are disk-shaped with approximately 9 nm in thickness and 100 nm in diameter. The crystallinity of nanomesas has been probed by x-ray diffraction and their ferroelectricity also has been shown by various measurements. The ferroelectric to paraelectric phase transition has been measured by temperature-dependent X-ray diffraction and macroscopic dielectric ‘butterfly’ hysteresis curves and pyroelectric hysteresis loops also have been observed from nanomesas.

Piezoresponse Force Microscopy (PFM) and PFM switching spectroscopy (SSPFM) are excellent tools for the purpose [1]. Previous studies of continuous LB films of ferroelectric polymers [2], revealed that the imaging resolution is below 5 nm, and well-behaved local polarization switching was also observed by obtaining piezoelectric hysteresis loops from regions of the film averaging 25-50 nm in size with SSPFM.

Here we report the preliminary results of local electromechanical characterization of ferroelectric polymer nanomesas [3] using PFM and SSPFM. Poling nanomesas over an area 600 nm square was successfully executed by applying a DC bias of  $\pm 7$  V to the PFM tip during scanning. Polarization switching loops were obtained by SSPFM over a region of 30 nm square. Some amount of modification of mesas morphology during scanning is, however, inevitable since the morphology of nanomesas itself introduces a rough, compliant surface to the probing tip. The results clearly demonstrate PSM imaging and switching with individual nanomesas.

Work at the Oak Ridge National Laboratory was supported by Laboratory Directed Research and Development funds. Work at the University of Nebraska was supported by the National Science Foundation and the Nebraska Research Initiative.

### References

- [1] S. V. Kalinin, A. Rar, S. Jesse. IEEE Trans. Ultrasonics Freq. Control **53**, 2223-52 (2007).
- [2] B. J. Rodriguez, S. Jesse, S. V. Kalinin, J. Kim, S. Ducharme, Appl. Phys. Lett. **90**, 122904 (2007).
- [3] M. Bai and S. Ducharme, Appl. Phys. Lett. **85**, 3528-30 (2004).

# Spectroscopic and Density Functional Theory Studies of Vinylidene Fluoride Oligomers

J. Travis Johnston,<sup>1</sup> Jihee Kim,<sup>1</sup> Rafal Korlacki,<sup>1</sup> Stephen Ducharme,<sup>1</sup>  
Zhongxin Ge,<sup>2</sup> James M. Takacs<sup>2</sup>

<sup>1</sup>Department of Physics and Astronomy

<sup>2</sup>Department of Chemistry

Nebraska Center for Materials and Nanoscience

University of Nebraska, Lincoln, NE 68588

E-mail: sducharme1@unl.edu

Thin films of vinylidene fluoride ( $\text{CH}_2\text{CF}_2$ ) oligomers [1] prepared by the Langmuir-Blodgett deposition on silicone substrates were investigated by comparing experimental and theoretical infrared spectra of oligomers with the structure  $\text{CF}_3 - (\text{CH}_2\text{CF}_2)_n - \text{I}$ . The experimental spectra were obtained from oligomers VDF count  $n = 14$  using the infrared spectroscopic ellipsometry combined with Lorentz oscillator analysis. Theoretical spectra were calculated for VDF count  $n = 8$  using the density functional theory. Excellent correspondence of major infrared bands in both datasets (Fig. 1) shows that the molecules are oriented with their long axes normal to the substrate plane, while in case of polyvinylidene fluoride Langmuir-Blodgett films the polymer chains are parallel to the substrates.

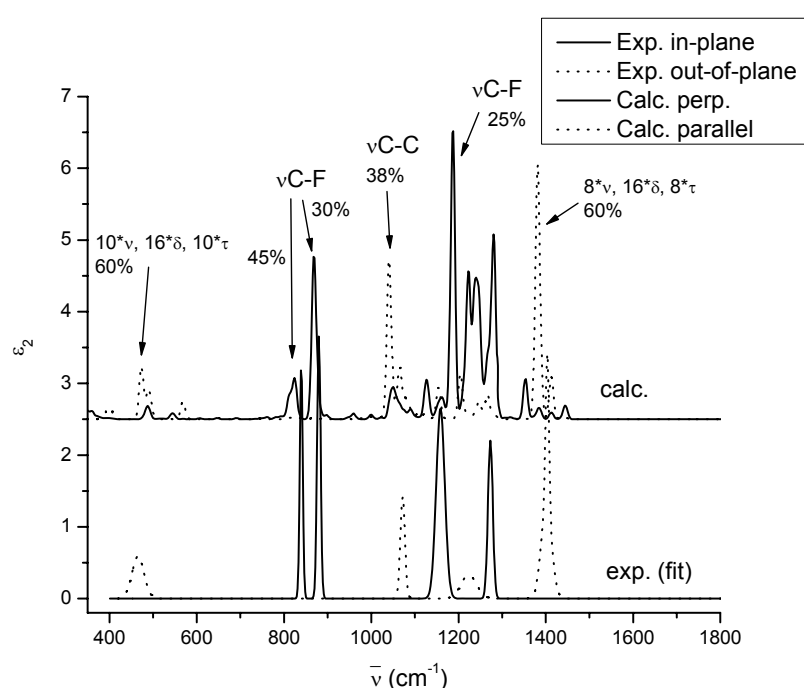


**Figure 1.** Infrared attenuation spectra from density functional theory (top) and ellipsometry (bottom).

The molecular conformation of the oligomers is consistent with the all-trans conformation of the ferroelectric form of polyvinylidene fluoride. The results of density functional theory calculations allow verification of empirical band assignments and force fields of vinylidene fluoride-based oligomers and polymers, widely present in the literature.

This work was supported by the Nebraska Research Initiative.

[1] K. Noda, K. Ishida, T. Horiuchi, K. Matsushige, A. Kubono, J. Appl. Phys. **86**, 3688 (1999).

# Apparatus for Pyroelectric Scanning Microscopy

Stella Stephens,<sup>1</sup> Horatio Vasquez,<sup>1</sup> Jihee Kim,<sup>2</sup> Stephen Ducharme<sup>2</sup>

<sup>1</sup>*Department of Mechanical Engineering*

*University of Texas – Pan American; Edenburg, TX 78539; E-mail: vasqu002@utpa.edu*

<sup>2</sup>*Department of Physics and Astronomy; Nebraska Center for Materials and Nanoscience  
University of Nebraska, Lincoln, NE 68588; E-mail: sducharme1@unl.edu*

Pyroelectric Scanning Microscopy (PSM) has been developed to enable mapping of surface polarization in ferroelectric capacitors. Images of the spatial distribution of pyroelectric response are obtained by scanning a focused and modulated laser beam across the sample and recording the resulting current modulation generated by the pyroelectric response, the change in polarization with change in temperature. The PSM images are in effect images of the polarization distribution because the pyroelectric response is proportional to net polarization [1]. We have improved on earlier versions of the method [2] by upgrading the critical components. A nanopositioning system provides repeatable positioning to approximately 5 nm. Switching from a red helium-neon laser source (633 nm wavelength) to a blue diode laser source (405 nm) and employing high-numerical-aperture microscope objectives should improved the optical resolution to less than 200 nm. The final critical improvement is to change the laser modulation method from mechanical chopping wheel (4 kHz) with direct laser modulation at frequencies up to 5 MHz to reduce the thermal diffusion length below the optical resolution. Preliminary results with a 0.65 N.A. microscope objective and 500 kHz modulation frequency produced repeatable PSM images with a resolution of 500 nm. The microscopy should realize a resolution of 150 nm can be achieved with an immersion objective. Additional capabilities include the ability to image polarization states at any point on the hysteresis loop, and to obtain time-dependent images of polarization switching dynamics [2].

This work was supported by the National Science Foundation through the Q-SPINS Materials Research Science and Engineering Research Center and by the University of Nebraska office of Graduate Studies.

## References

- [1] A. V. Bune, C. Zhu, S. Ducharme, L. M. Blinov, V. M. Fridkin, S. P. Palto, N. N. Petukhova, S. G. Yudin, *J. Appl. Phys.* **85**, 7869-73 (1999).
- [2] I. F. Faria Jr., C. C. Ghizoni, and L. C. M. Miranda, *Appl. Phys. Lett.* **47**, 1154-6 (1985). S. Yilmaz, S. Bauer, W. Wirges, and R. Gerhard-Multhaupt, *Appl. Phys. Lett.* **63**, 1724 (1993). B. Peterson, S. Ducharme, V. M. Fridkin, T. J. Reece, *Ferroelectrics* **304**, 51-54 (2004).

# Effect of Ferroelectric Polarization on Tunneling Current

Evgeny Kiriranov<sup>1</sup>, Jody Redepenning<sup>2,3</sup> and Andrei Sokolov<sup>3,4</sup>

<sup>1</sup>Lincoln South-West High School, 7001 South 14<sup>th</sup>, Lincoln, NE, 68512

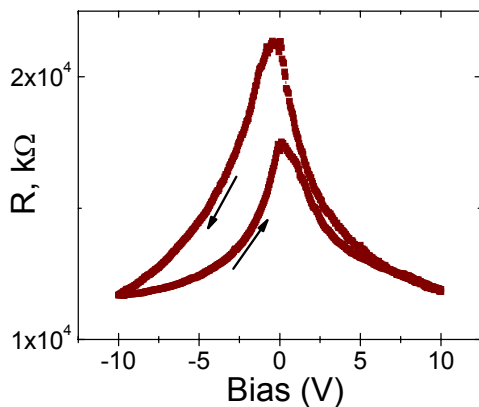
<sup>2</sup> Department of Chemistry, University of Nebraska-Lincoln, Lincoln, NE 68588

<sup>3</sup> Nebraska Center for Materials and Nanoscience, University of Nebraska, Lincoln, NE 68588

<sup>4</sup> Department of Physics and Astronomy, University of Nebraska, Lincoln, NE 68588

E-mail: asokol@unlserve.unl.edu

In the recent years electron transport through organic materials drew a great deal of attention due to large variety of interesting properties relevant for design of new electronic devices. One attractive example of such properties is the observance of ferroelectric effect in P(VDF-TrFE) organic co-polymer<sup>1</sup>. On the other hand, the use of a thin ferroelectric film as tunnel barrier is predicted to significantly expand the functionality of commonly used tunnel junctions<sup>2</sup>. However, experimental realization of organic based tunnel junctions face a major difficulty due to extreme fragility of such thin film to patterning of metal electrodes. Thus, for experimental observation of the effect of ferroelectric P(VDF-TrFE) on tunnel transport and to clarify the actual mechanism of electroresistance a new experimental setup, different to standard ‘pillar’ geometry has to be realized.



We present the results of study of the electron transport through ferroelectric co-polymer P(VDF-TrFE). First, nano-gap was formed, using controlled breaking of a Au nanowire to form a nanogap and then filled by the polymer from a solution under an orientation potential. Current –voltage character, presented on Fig.1, reveals a hysteretic behavior, a signature of the effect of ferroelectric polarization on resistance of the tunnel junction. Possible interpretations of the effect will be discussed.

**Figure 1.** Resistance as a function of applied bias voltage for a tunnel junction with organic polymer Au/P(VDF-TrFE)/Au co-polymer.

## References

- [1] A. Bune, V. M. Fridkin, S. Ducharme, L. M. Blinov, S. P. Palto, A. Sorokin, S. G. Yudin, A. Zlatkin “Two-Dimensional Ferroelectric Films”, *Nature* **391**, 874-877 (1998).
- [2] E. Y. Tsymbal and H. Kohlstedt, “Tunneling across a ferroelectric”, *Science* **313**, 181-183 (2006).

## Activated Water Desorption from Poly(vinylidene fluoride with trifluoroethylene) and Poly(methylvinylidene cyanide)

**Carolina C. Ilie<sup>1</sup>, P. A. Jacobson<sup>1</sup>, I. N. Yakovkin<sup>2</sup>, Luis. G. Rosa<sup>1</sup>, Jie Xiao<sup>1</sup>, Matt Poulsen<sup>1</sup>, D. Sahadeva Reddy<sup>3</sup>, James M. Takacs<sup>3</sup>, and P. A. Dowben<sup>1</sup>**

<sup>1</sup>*Dept. of Physics and Astronomy, University of Nebraska - Lincoln, Lincoln, NE, USA.*

<sup>2</sup>*Institute of Physics of National Academy of Sciences of Ukraine, Kiev, Ukraine.*

<sup>3</sup>*Dept. of Chemistry, University of Nebraska - Lincoln, Lincoln, NE, USA.*

*E-mail: cilie@unlserve.unl.edu*

Activated desorption processes have been previously suggested, but the microscopic mechanisms have not been directly identified. In polymer systems, examples of both extrinsic and intrinsic activated molecular desorption may be found. In comparing water desorption from the ferroelectric copolymer poly(vinylidene fluoride-trifluoroethylene), and water desorption from the dipole ordered polymer poly(methylvinylidene cyanide), we find that extrinsic activation of water desorption is possible from the former, and intrinsic activation of water desorption is possible from the latter. The angle resolved thermal desorption spectra show large deviations from the expected  $\cos^{\beta}\theta$  distribution [1,2] for light illuminated poly(vinylidene fluoride-trifluoroethylene). Water desorption from poly(methylvinylidene cyanide) deviates from the  $\cos^{\beta}\theta$  distribution without illumination [3].

Both films, prepared by the Langmuir Blodgett technique from a water subphase, exhibit good surface crystallinity, as determined by STM and band structure [4]. The thermal desorption spectra indicate that the absorbed water species interacts more strongly with poly(vinylidene fluoride-trifluoroethylene) than with poly(methylvinylidene cyanide).

The absorption of water is believed to distort the polymer chain placement for both polymers [5]. The Arrhenius plots obtained from Polanyi-Wigner analysis of the thermal desorption data suggest that a two states model of desorption applies to poly(methylvinylidene cyanide), while theory suggests that strain plays a key role in the water desorption process from this polymer [6]. Strain effects are seen when there is restricted dipole motion: dipole motion is important.

1. Comsa, G.; David, R.; Rendulic, K. D., Phys. Rev. Lett. **38**, 775, 1977.
2. Steinrück, H. P., Winkler, A., Rendulic, K. D., J. Phys. C: Solid State Phys. **17**, L311, 1984.
3. Ilie, Carolina C.; Jacobson, P. A.; Yakovkin, I. N.; Rosa, Luis G.; Poulsen, M., Sahadeva Reddy, D.; Takacs, James M.; P.A. Dowben, J. Phys. Chem. B **111**, 7742-7746, 2007.
4. Xiao, Jie; Rosa, Luis G.; Poulsen, M.; Feng, D.-Q.; Sahadeva Reddy, D.; Takacs, J. M.; Cai, Lei; Zhang, Jiandi; Ducharme, S.; Dowben, P. A., J. Phys. Cond. Matter **18**, L155, 2006.
5. Jacobson, P. A.; Ilie, Carolina C.; Yakovkin, I. N.; Poulsen, M.; Sahadeva Reddy, D.; Takacs, J. M.; Ducharme, S.; Dowben, P. A., J. Phys. Chem. B **110**, 15389, 2006.
6. Dowben, P. A.; Rosa, L. G.; Ilie, Carolina C. submitted to Zeitschrift für Physikalische Chemie.

## Stabilizer-free Nanostructured Zirconia

Gonghua Wang<sup>1</sup>, Chin Li Cheung<sup>1</sup>, Fereydoon Namavar<sup>2</sup>, Jaeil Bai<sup>1</sup>,  
Renat F. Sabirianov<sup>3</sup>, Xiao Cheng Zeng<sup>1</sup>, Joseph R. Brewer<sup>1</sup>, Wai -Ning  
Mei<sup>3</sup>, Hani Haider<sup>2</sup> and Kevin L. Garvin<sup>2</sup>

<sup>1</sup>*Department of Chemistry and Nebraska Centre for Materials and Nanoscience,  
University of Nebraska-Lincoln, Lincoln, NE 68588.*

<sup>2</sup>*Department of Orthopaedic Surgery and Rehabilitation, University of Nebraska-Medical  
Center, Omaha, NE 68198.*

<sup>3</sup>*Department of Physics, University of Nebraska-Omaha, Omaha, NE 68182.  
E-mail: gwang@bigred.unl.edu*

Zirconia (ZrO<sub>2</sub>) has been an important ceramic material because of their superior mechanical, optical and chemical properties. [1, 2] The most common phases of zirconia are monoclinic, tetragonal and cubic phase [3, 4]. Monoclinic ZrO<sub>2</sub> is thermodynamically stable at room temperature, whereas the tetragonal and cubic phases are stable at much higher temperatures. To obtain the metastable cubic phase zirconia at room temperature, traditionally, addition of trivalent stabilizers such as ceria and yttria are necessary. Nevertheless, these stabilizers can deteriorate the mechanical properties of these materials [4]. Hence we design and fabricate nanostructurally stabilized zirconia films without chemical stabilizers by the ion beam assisted deposition technique [5]. Rutherford backscattering spectroscopy confirmed the formation of stoichiometric ZrO<sub>2</sub>. X-ray diffractometry and selected area electron diffraction results further verified that the as-deposited films at room temperature are consistent with cubic phase of zirconium oxide. Mixed-phase ZrO<sub>2</sub> films produced at higher deposition temperatures exhibit triangular hillock structures. These films have both merits of high hardness and complete wettability with water (contact angles of zero to several degrees). Thus the biocompatible zirconia films can potentially benefit biomedical applications where hard and hydrophilic coatings are desired. The Wenzel model [6] will be employed to explain the hydrophilic behavior of these films.

### References

- [1] R. C. Garvie, R. H. Hannink, R. T. Pascoe, "Ceramic Steels?", *Nature* **258**, 703-704 (1975).
- [2] G. D. Wilk, R. M. Wallace, J. M. Anthony, "High-k gate dielectrics: Current status and materials properties considerations", *J. Appl. Phys.* **89**, 5243-5275 (2001).
- [3] R. C. Garvie, P. S. Nicholson, "Phase analysis in zirconia systems", *J. Am. Ceram. Soc.* **55**, 303-305 (1972).
- [4] C. Piconi, G. Maccauro, "Zirconia as a ceramic biomaterial", *Biomaterials* **20**, 1-25 (1999).
- [5] P. Martin, "Ionization-assisted evaporative processes: techniques and film properties", *IEEE T. Plasma Sci.* **18**, 855-868(1990).
- [6] R. N. Wenzel, *Ind. Eng. Chem.* **28**, 988-994 (1936).

## Polarized and Time-resolved Photoluminescence Measurements of Single Zincblende and Wurtzite InP Nanowires

**J. M. Yarrison-Rice<sup>1</sup>, A. Mishra<sup>2</sup>, T.B. Hoang<sup>2</sup>, L.V. Titova<sup>2</sup>, L.M. Smith<sup>2</sup>, H.E. Jackson<sup>2</sup>, H.J. Joyce<sup>3</sup>, H.H. Tan<sup>3</sup>, and C. Jagadish<sup>3</sup>**

<sup>1</sup>*Physics Department, Miami University, Oxford, OH 45056*

<sup>2</sup>*Department of Physics, University of Cincinnati, Cincinnati, OH 45221*

<sup>3</sup>*Department of Electronic Materials Engineering, Australian National University,  
Canberra, ACT 0200*

*E-mail: yarrisjm@muohio.edu*

Semiconductor nanowires are rapidly becoming essential components in a variety of novel nanoscale devices.[1,2] Design optimization of such structures requires a solid understanding of how the electronic and optical properties are influenced by the various growth parameters. Semiconductor InP nanowires grown by the gold-catalyzed vapor liquid solid mechanism exhibit Zincblende (cubic) stoichiometry when grown at lower temperatures (420 C) and Wurtzite (hexagonal) structure at growth temperatures of 480 °C.

Polarized PL spectroscopy of single NW shows dramatically different behavior between the Zincblende and Wurtzite forms. While at low temperatures (20K) the Zincblende nanowire exhibits the same spectral position (1.42 eV) as seen in a comparison epilayer grown under optimal conditions, the hexagonal Wurtzite NW exhibits a PL peak which is 70 meV higher in energy at 1.49 eV. The cubic NW is strongly polarized along the NW axis because of the dielectric discontinuity. The hexagonal Wurtzite NW exhibits strongly polarized emission *perpendicular* to the NW axis indicating that the c-axis is along the NW axis. We have used time resolved PL to study the dynamics of electrons and holes confined to the cubic 420 C InP NWs.[3] After excitation with a 200 fs laser pulse at 780 nm, we observe a broad emission in short times after excitation consistent with the production of a high density degenerate electron-hole plasma which cools over a few hundred picoseconds to an emission centered on the free exciton line.

### References

- [1] F. Patolsky, G. Zheng, and C.M. Lieber, „Nanowire-based biosensors,” *Anal. Chem.* **78**, 4260-4269 (2006).
- [2] A.B. Greytak, C.J. Barrelet, Y. Li, and C.M. Lieber, „Semiconductor nanowire laser and nanowire waveguide electro-optic modulators,” *Appl. Phys. Lett.* **87**, 151103[1-3] (2005).
- [3] L.B. Titova, T.B Hoang, J.M. Yarrison-Rice, H.E. Jackson, Y. Kim, H.J. Joyce, Q. Gao, H.H. Tan, C. Jagadish, X. Zhang, J. Zou, and L.M. Smith, “Dynamics of strongly degenerate electron-hole plasmas and excitons in single InP nanowires,” Accepted for publication by *Nanoletters*, (2007).

# Investigation of Single CdS Nanosheets with Spatially-, Temporally-, and Polarization-resolved Photoluminescence

**H. E. Jackson<sup>1</sup>, K.-Y. Lee<sup>3</sup>, H. Rho<sup>3</sup>, L. V. Titova<sup>1</sup>, T. B. Hoang<sup>1</sup>,  
A. Mishra<sup>1</sup>, L. M. Smith<sup>1</sup>, J. M. Yarrison-Rice<sup>2</sup>, Y.-J. Choi<sup>4</sup>, K.-J. Choi<sup>4</sup>,  
and J.-G. Park<sup>4</sup>**

<sup>1</sup>*Department of Physics, University of Cincinnati, Cincinnati, Ohio 45221 USA*

<sup>2</sup>*Department of Physics, Miami University, Oxford, Ohio 45056 USA*

<sup>3</sup>*Department of Physics, Chonbuk National University, Jeonju 561-756, Korea*

<sup>4</sup>*Nano Materials Research Center, Korea Institute of Science and Technology,  
Seoul 130-650, Korea*

*E-mail: howard.jackson@uc.edu*

CdS nanowires[1-2] and nanosheets [3] (II-VI semiconductor materials) are rapidly finding application in various novel photonic and electronic devices. Nanosheets are of particular interest because they have micron dimensions in length and width, with ~40 nm thicknesses, which could make them useful for different device structures. We describe results which combine high resolution TEM, polarization dependent photoluminescence (PL), with spatial and temporally resolved PL measurements to provide a more comprehensive understanding of the electronic and crystalline structure of these CdS nanosheets. The highly crystalline CdS nanosheets were grown by pulsed laser deposition. Polarized PL as a function of angle is measured and provides the orientation of the c-axis relative to the nanosheet growth direction.

Recombination lifetimes of excitons confined to single CdS nanosheets were recorded using time-resolved PL.[3] The lifetimes were seen to be significantly longer than observed in CdS nanowires, presumably because surface recombination is significantly reduced in these large 2D structures. Low temperature spatially-resolved PL measurements were recorded from several nanosheets. The total integrated emission intensity is similar along the entire sheet, but the intensities vary significantly for different emission peaks as a function of position across the nanosheet. Such a variation may indicate variation in strain across the width of the sample.

- [1] T.B. Hoang, L.V. Titova, J.M. Yarrison-Rice, H.E. Jackson, L.M. Smith, J.L. Lensch, and L.J. Lauhon, "Temperature dependent photoluminescence of single CdS nanowires," *Appl. Phys. Lett.* **89**, 123123-1-3 (2006).
- [2] L.V. Titova, T.B. Hoang, J.M. Yarrison-Rice, H.E. Jackson, L.M. Smith, J.L. Lensch, and L.J. Lauhon, "Low temperature photoluminescence imaging and time-resolved spectroscopy of single CdS nanowires," *Appl. Phys. Lett.* **89**, 053119-1-3 (2006).
- [3] H. Rho, T.B. Hoang, L.V. Titova, K.-Y. Lee, A. Mishra, J.M. Yarrison-Rice, Y.-J. Choi, K. Choi, J.-G. Park, L.M. Smith and H.E. Jackson, "Spatially-resolved photoluminescence mapping of single CdS nanosheets," Submitted to *Nanoletters* August 2007.

## Growth of Crystalline Lanthanum Hexaboride Nanostructures

Joseph R. Brewer<sup>†</sup>, Nirmalendu Deo<sup>†</sup> and Chin Li Cheung<sup>†,‡</sup>

<sup>†</sup>*Department of Chemistry, University of Nebraska-Lincoln, Lincoln, Nebraska 68588*  
and, <sup>‡</sup>*Nebraska Center for Materials and Nanoscience, Lincoln, Nebraska 68588.*  
*E-mail: ccheung2@unl.edu*

Low work function high aspect ratio materials are of great importance for the development of energy efficient field-induced electron emitters. Lanthanum hexaboride (LaB<sub>6</sub>) is among one of the known materials with high thermal stability, low work function and high electron emissivity [1]. Though the synthesis of LaB<sub>6</sub> nanowires has been reported in the literature [2] [3], the shape and tip diameter control of robust LaB<sub>6</sub> nanostructures is lacking. Here, we report our development of a low temperature chemical vapor deposition process for the growth of single crystalline LaB<sub>6</sub> nanoobelisks and nanowires from B<sub>10</sub>H<sub>14</sub> and LaCl<sub>3</sub> precursor materials. Growth of these obelisks and wires was preferentially obtained by the appropriate choice of catalyst particles, temperature of reaction and precursor flux. Diameters of the nanoobelisk tips are  $11 \pm 5$  nm. The nanowire diameters range from 30 to 40 nm. High resolution TEM indicated a preferred (100) growth direction and single-crystallinity for these nanomaterials. The preferential shape growth mechanism of these different nanostructures and their applications in nanoelectronics will be discussed.

### References

- [1] Kore Technology. AP Tech Electron Sources. 23 July 2007. 15 Aug. 2007  
<<http://www.kore.co.uk/aptech.htm#life>>.
- [2] H. Zhang, J. Tang, Q. Zhang, G. Zhao, G. Yang, J. Zhang, O. Zhou, L.-C. Qin, "Field emission of electrons from single LaB<sub>6</sub> nanowires", *Adv. Mater.* **18**, 87-91 (2006).
- [3] J. Xu, Y. Zhao, C. Zou, "Self-catalyst growth of LaB<sub>6</sub> nanowires and nanotubes", *Chem. Phys. Lett.* **423**, 138-142 (2006)

# The Elastic Constants and Related Mechanical Properties of the Monoclinic Polymorph of the Carbamazepine Molecular Crystal

Himansu Mohapatra and Craig J. Eckhardt

*Department of Chemistry, Nebraska Center for Materials and Nanoscience, University of Nebraska-Lincoln, Lincoln, Nebraska 68588-0304.  
E-mail: mohapatr@unlserve.unl.edu*

Mechanical properties of pharmaceuticals are critical to their processing for deliverable forms of dosage. Brillouin scattering has been used to probe the acoustic phonons of the monoclinic ( $P2_1/c$ ) polymorph of the drug, carbamazepine (CBZ III). By sampling a variety of acoustic phonons, the complete elastic constant tensor has been determined for this CBZ polymorph. A representative Brillouin spectrum of CBZ III is shown in Figure 1. The diagonal elastic constants  $c_{11}$ ,  $c_{22}$ ,  $c_{33}$ ,  $c_{44}$ ,  $c_{55}$  and  $c_{66}$  are 10.89 GPa, 11.47 GPa, 11.32 GPa, 3.68 GPa, 0.85 GPa and 2.89 GPa respectively. The elastic constants of CBZ III are effectively governed by non-directed dispersive type interactions similar to aromatic systems with delocalized  $\pi$ -bonds. The bulk modulus and linear compressibility have been calculated from the compliance matrix. The relative strength of intermolecular interactions in different directions is deduced from linear compressibility plots for three crystallographic planes. Cauchy's ratio, calculated from the elastic constants, suggests that many-body interactions in CBZ III contribute significantly to the lattice anharmonicity.

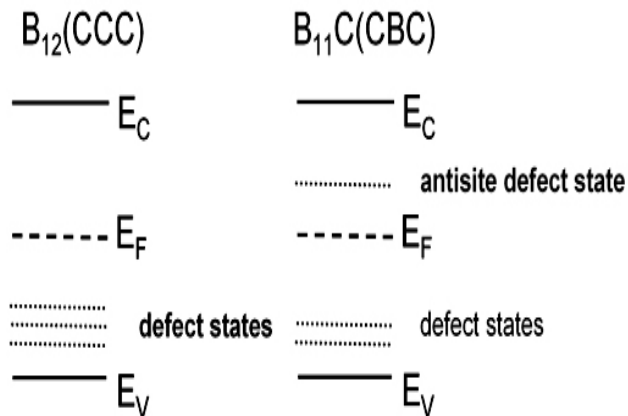
# The Role of Defects in Amorphous Hydrogenated Boron Carbide $a\text{-B}_5\text{C:H}$

M. Sky Driver and A. N. Caruso

*Department of Physics, University of Missouri-Kansas City  
E-mail: msdriver@umkc.edu*

With the absence of long range order, multiple short range/coordination environments and interstitial hydrogen found for low temperature deposited boron carbide (BC), many distinct electronic polytypes are present. Specifically, it is the local structural defects in this electron poor (boron rich) solid that dictate the majority carrier, transport character, as well as gap magnitude; all of which can be tuned/changed by the initial growth conditions. For high pressure/temperature grown  $\text{B}_4\text{C}$ , Schmechel and Werheit state that in their crystalline state, the boron-rich solids represent a brilliant insulator where only through defects may the solid go toward a semiconducting state [1].

In the case of low temperature depositions reported here, the defects may also be controlled by the precursor type, namely through the carborane isomers: orthocarborane and metacarborane. Previous results [2,3] find that the orthocarborane based  $a\text{-B}_5\text{C:H}$  results in a stable p-type solid, while the metacarborane yields an n-type material; recent studies demonstrate that the metacarborane based solid reverts to p-type upon thermal treatment. It is interesting to note that in the case of high temperature based  $\text{B}_4\text{C}$ , no hydrogen is present; this then calls into question the role of hydrogen in the low temperature deposited material with regard to defect formation and/or passivation.



From a basic view, understanding the structural differences that result in the various electronic properties, that is, intrinsic doping, is important in general for the semiconductor community. From an applied stance, understanding how we may control and reproduce such defects is important for solid state voltaic devices, role of defects electronically and how they are manifest structurally.

## References

- [1] R Schmechel and H Werheit, "Correlation between Structural Defects and electronic Properties of Icosahedral Boron-Rich Solids". *J. Phys. Condensed Matter*. **11**, 6803-6813 (1999).
- [2] A. N. Caruso and et al., "Surface photovoltage effects on the isomeric semiconductors of boron-carbide". *Applied Physics Letters*. Volume **84** Number 8 1302-1304 (2004).
- [3] A. N. Caruso and et al., "The heterisomeric diode". *J. Phys. Condensed Matter*. **16**, L139-L146 (2004).

## The Bulk Band Structure and Inner Potential of Layered $\text{In}_4\text{Se}_3$

**Jing Liu,<sup>1,a</sup> Ya. B. Losovyj,<sup>1,2,b</sup> T. Komesu,<sup>1,c</sup> P. A. Dowben,<sup>1,d</sup> L. Makinistian,<sup>3,e</sup> E. A. Albanesi,<sup>4,f</sup> Andre Petukhov,<sup>5,g</sup> P. Galiy,<sup>6,h</sup> Ya. Fiyala<sup>6</sup>**

<sup>1</sup> *Dept. of Physics and Astronomy and the Nebraska Center for Material and Nanoscience, University of Nebraska, Lincoln, NE 68588, USA*

<sup>2</sup> *Louisiana State University, CAMD, Baton Rouge, LA, USA*

<sup>3</sup> *Facultad de Ingeniería, Universidad Nacional de Entre Ríos, 3101 Oro Verde (ER), Argentina*

<sup>4</sup> *INTEC-CONICET, Güemes 3450, 3000 Santa Fe, Argentina*

<sup>5</sup> *South Dakota School of Mines, Department of Physics, Rapid City, South Dakota 57701-3995, USA*

<sup>6</sup> *Electronics Dept., Lviv National University, 50 Dragomanov Str., 79005 Lviv, Ukraine*

<sup>a</sup> *jingliu@bigred.unl.edu,* <sup>b</sup> *ylosovyj@lsu.edu,* <sup>c</sup> *tkomesu@spring8.or.jp,*

<sup>d</sup> *pdowben@unlinfo.unl.edu,* <sup>e</sup> *lmakinistian@ceride.gov.ar,* <sup>f</sup> *eea@intec.ceride.gov.ar,*

<sup>h</sup> *galiy@electronics.wups.lviv.ua*

The band structure of the layered  $\text{In}_4\text{Se}_3$  system was studied by angled-resolved photoemission (ARPES). Both bulk and surface features were identified through photon energy dependent ARPES. The surface state dispersions were measured in  $\Gamma$ -X and  $\Gamma$ -Y directions. Band widths (the extent of dispersion) of 300 meV or more are observed, for In-p and Se-p weighted bands within the valence region with changing photon energy, and is indicative of a bulk band structure perpendicular to the cleavage plane. Two-dimensionality of state is clearly not conserved, and there must exist interactions between layers sufficient to support a bulk band structure. The cleavage surfaces are ordered with the critical points consistent with LEED.

## Comparison of Electric Properties of Boron Carbide and N-Doped Boron Carbide

**Nina Hong, Ravi Billa\* and Shireen Adenwalla**

*Department of Physics, University of Nebraska-Lincoln, Lincoln, NE 68588-0511, USA*

*\*Department of Mechanical Engineering, University of Nebraska-Lincoln, Lincoln, NE 68588-0511, USA*

*E-mail: ninahong@bigred.unl.edu*

The development of a semiconducting form of boron carbide by plasma-enhanced chemical-vapor deposition (PECVD) here at UNL has led to the development of neutron detectors and semiconductor devices based on this unusual semiconductor. Here we study the effects of doping. Boron carbide ( $B_5C$ ) and Ni-doped boron carbide ( $Ni-B_5C$ ) films were fabricated on silicon wafers by PECVD. Current-Voltage (I-V) characteristics at room temperature showed that  $B_5C$  and  $Ni-B_5C$  were p-type and n-type semiconductors, with respectable diode characteristics. Capacitance-Voltage (C-V) measurement at 10 kHz showed that these heterojunction diodes had abrupt junctions and depletion widths of  $2.7\mu m$ . Similar films of  $B_5C$  and  $Ni-B_5C$  were also grown on sapphire substrates for resistivity measurements, resulting in values of  $10^{10} \Omega cm$  for the  $B_5C$  film and  $10^8 \Omega cm$  for the  $Ni-B_5C$  film at room temperature. The dielectric constant was estimated by capacitance measurement of these resistive layers, showing that both  $B_5C$  and  $Ni-B_5C$  films had the dielectric constants of 10.

ACKNOWLEDGEMENT : Funded by NASA under the ASTID program Grant Number NNG05GM89G

# Nd<sup>3+</sup>-Doped Titania Nanotubes

Wanwan Huang<sup>1</sup>, Dilip K. Paul<sup>2</sup>, and Chin Li Cheung<sup>1</sup>

<sup>1</sup>*Department of Chemistry and Nebraska Centre for Materials and Nanoscience,  
University of Nebraska-Lincoln, Lincoln, NE 68588*

<sup>2</sup>*Department of Chemistry, Pittsburg State University, 1701 South Broadway, Pittsburg  
KS 66762*

*E-mail: ccheung2@unl.edu*

The photocatalytic decomposition of organic pollutants in water and air has attracted much interest for decades due to its potential as an effective means to clean up environmental pollution. Among various semi-conducting materials, anatase titanium dioxide (TiO<sub>2</sub>) has been given the most attention because of its high photocatalytic activity, photostability, low-toxicity, and low cost. However, since it has a large band gap (3.2eV), only a small fraction of solar light (UV) can be utilized for the catalytic reaction.

Titania nanotubes (TNTs) are potentially a better choice than TiO<sub>2</sub> particles because the morphology and tubular structures of TNTs allow for less efficient packing in bulk form, which in turn, allow for more catalytic sites and exposed reactive surface areas. TNTs have been previously prepared by hydrothermal reactions from anatase in 10 M NaOH solution at 140 °C [1]. We devised a modified synthesis method which allows the preparation of TNTs decorated with neodymium ions (Nd<sup>3+</sup>) in a one-step synthesis [2]. Transmission electron microscopy studies revealed that the nanotubes are several hundred nanometers long with an average diameter of 20 nm. The as-prepared Nd<sup>3+</sup>-doped TNTs are expected to show a narrower band gap than pure TNTs because the 4f orbitals of Nd<sup>3+</sup> forming the new conduction energy levels allowing for a larger range of solar light to be utilized. We performed the photocatalytic degradation of acetaldehyde over pure TNTs under UV light according to the literature procedure [3]. The FTIR spectra of our results indicate that H<sub>2</sub>O, CO<sub>2</sub>, and COO<sup>-</sup> groups are generated during the reaction.

## References

- [1] T. Kasuga, M. Hiramatsu, A. Hoson, T. Sekino, and K. Niihara, "Formation of titanium oxide nanotube", *Langmuir* **14**, 3160-3163 (1998).
- [2] E.Y. Kim, Y.H. Kim, and C.M. Whang, "Nd<sup>3+</sup>-doped TiO<sub>2</sub> nanoparticles prepared by sol-hydrothermal process", *Mater. Sci. Forum*, **510-511**, 122-125 (2006).
- [3] D.A. Panayotov, D.K. Paul, and J.T. Yates, Jr, "Photocatalytic oxidation of 2-chloroethyl ethyl sulfide on TiO<sub>2</sub>-SiO<sub>2</sub>", *J. Phys. Chem. B* **107**, 10571-10575 (2003).

## Polarization Coupled Response of ZnO-BaTiO<sub>3</sub> Heterojunctions: A Model Approach.

V. M. Voora<sup>1</sup>, T. Hofmann<sup>1</sup>, M. Brandt<sup>2</sup>, M. Lorenz<sup>2</sup>, M. Grundmann<sup>2</sup>,  
and M. Schubert<sup>1</sup>

<sup>1</sup>*Department of Electrical Engineering and Nebraska Center for Materials and Nanoscience, University of Nebraska-Lincoln, U.S.A.*

<sup>2</sup>*Institut für Experimentelle Physik II, Universität Leipzig, 04103 Leipzig, Germany  
E-mail: vvoora1@bigred.unl.edu*

Heterojunctions composed of wurtzite-structure ZnO and perovskite-structure (ferroelectric) BaTiO<sub>3</sub> are very interesting because of the previously observed ionic lattice polarization coupling at their interfaces [1, 2]. We will report electric Sawyer-Tower polarization hysteresis measurements and analysis of a ZnO-BaTiO<sub>3</sub> heterostructure with Pt front and back contacts deposited by pulsed laser deposition onto a (001) silicon substrate. The ZnO layer is *n*-type, and the BaTiO<sub>3</sub> layer is highly resistive. We observe a strong asymmetric ferroelectric hysteresis, which we attribute to a rectifying depletion layer formation between the ZnO and BaTiO<sub>3</sub> layers. The coupling between the wurtzite-structure and perovskite-structure interface polarization influences the depletion layer formation. We develop a physical model for the electric Sawyer-Tower measurements. Our model includes the effects of the depletion layer formation inside the ZnO layer, the interface charge coupling between the ZnO and BaTiO<sub>3</sub> layers, and the field-dependent ferroelectric polarization inside the BaTiO<sub>3</sub>. We obtain a very good agreement between our model generated data and our experiment. The influence of physical model parameters on the ZnO-BaTiO<sub>3</sub> heterojunction characteristics will be discussed.

### References

- [1] N. Ashkenov, M. Schubert, E. Twerdowski, H. V. Wenckstern, B. N. Mbenkum, H. Hochmuth, M. Lorenz, W. Grill, and, M. Grundmann, *Thin solid Films*. **486**, 153, (2005).
- [2] B. N. Mbenkum, N. Ashkenov, M. Schubert, M. Lorenz, H. Hochmuth, D. Michel, M. Grundmann, and G. Wagner, *Appl. Phys. Lett.* **86**, 091904, (2005).

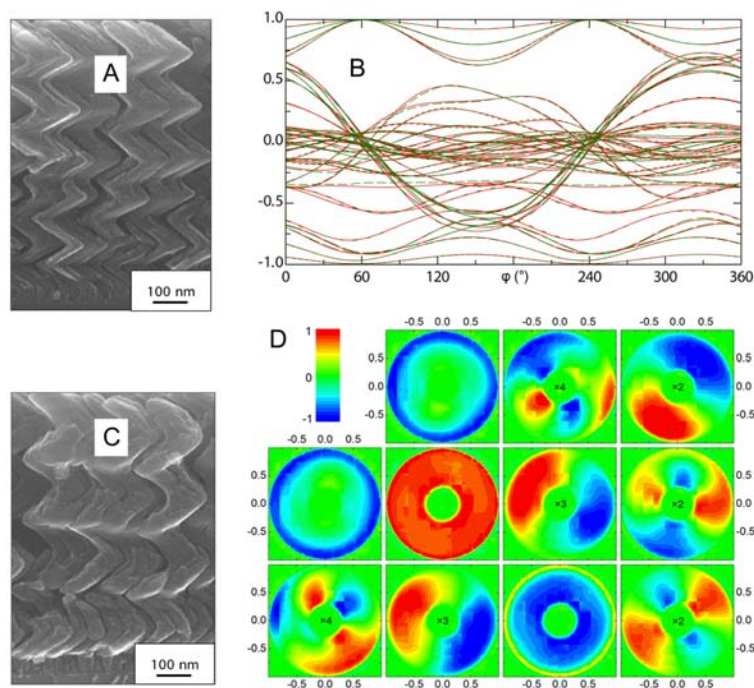
# Angle-Resolved Generalized Ellipsometry: Form-Birefringent Chiral and Achiral Silicon Sculptured Thin Films

D. Schmidt, E. Schubert, and M. Schubert

*Department of Electrical Engineering and Nebraska Center for Materials and  
Nanoscience, University of Nebraska-Lincoln, U.S.A.*

*E-mail: schmidt@bigred.unl.edu*

We report on generalized ellipsometry characterization of sculptured thin films (STFs). Samples are made from silicon by ion beam assisted deposition designed in geometries of columns, chevrons, left-handed multi-fold and continuous screws, with achiral and chiral properties. Intriguing form-birefringence-induced chirality and dielectric anisotropy are observed, highlighted, analyzed and quantified by azimuth and angle-of-incidence resolved reflection-type Mueller matrix ellipsometry. We discuss chirality, optical constants and symmetry assessment by generalized ellipsometry, and future research prospects.



Scanning electron micrographs of STF samples with chevron (A) and left-handed open three-fold screw (C) structures. Angle-resolved Mueller matrix ellipsometry ( $\lambda = 1550$  nm) data (red lines: best-match model; green lines: experiment) from the chevron sample (B). Color plots (D) of Mueller matrix (fourth row excluded) from the chiral structure in (C) versus in-plane angle  $\phi$  and angle of incidence  $\Phi_a$  ( $-1 \leq x = \sin \Phi_a \cos \phi \leq 1$ ,  $-1 \leq y = \sin \Phi_a \sin \phi \leq 1$ ).

## Nanoscale Observation of Delayering in Alkane Films

M. Bai<sup>1</sup>, K. Knorr<sup>1,2</sup>, H. Taub<sup>1</sup>, U. G. Volkmann<sup>3</sup>, and F. Y. Hansen<sup>4</sup>

<sup>1</sup>*Department of Physics and Astronomy and University of Missouri Research Reactor, University of Missouri-Columbia, Columbia, MO 65211*

<sup>2</sup>*Technische Physik, Universität des Saarlandes – D-66041 Saarbrücken, Germany*

<sup>3</sup>*Facultad de Física, Pontificia Universidad Católica de Chile – Santiago 22, Chile*

<sup>4</sup>*Department of Chemistry, Technical University of Denmark – IK 207 DTU, DK-2800 Lyngby, Denmark*

*E-mail: baime@missouri.edu*

Alkanes ( $n\text{-C}_n\text{H}_{2n+2}$ ) are of general interest as prototypes of more complex polymers used in coatings, adhesives, and electronic devices. They are also of interest as the building blocks of biologically important lipid molecules and as the principal constituents of commercial lubricants. Understanding their nanoscale growth and wetting behavior on solid surfaces is important for both fundamental studies and applications [1,2].

We have investigated the wetting behavior of alkane molecules of intermediate length ( $20 < n < 40$ ) adsorbed on  $\text{SiO}_2$  and graphite surfaces using Atomic Force Microscopy (AFM) and synchrotron x-ray scattering [3]. Tapping-mode AFM reveals a narrow temperature range (66–69 °C) near the bulk melting point  $T_b$  in which a monolayer phase of dotriacontane ( $n\text{-C}_{32}\text{H}_{66}$  or C32) molecules oriented perpendicular to surface is stable (Fig. 1). This monolayer phase undergoes a delayering transition to a three-dimensional (3D) fluid phase on heating to just above  $T_b$  and to a solid 3D phase on cooling below  $T_b$ .

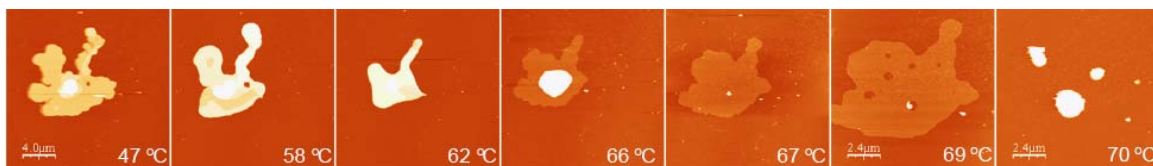


Figure 1. Topographic AFM images taken in the tapping mode on heating a low coverage C32 film: 3D solid particle (47–62 °C); 2D monolayer phase (66–69 °C); and 3D droplet (70 °C).

An equilibrium phase diagram provides a useful framework for interpreting the unusual spreading and receding of the monolayer observed in transitions to and from the respective 3D phases. AFM and synchrotron x-ray measurements indicate that a similar phase diagram applies to C32 deposited from solution onto a graphite surface as well as to a range of alkanes (C24 to C36) on  $\text{SiO}_2$  surfaces.

### References

- [1] P. G. de Gennes, “Wetting: statics and dynamics,” *Rev. Mod. Phys.* **57**, 827–863 (1985).
- [2] P. Lazar, H. Schollmeyer, and H. Riegler, “Spreading and two-dimensional mobility of long-chain alkanes at solid/gas interfaces,” *Phys. Rev. Lett.* **95**, 136103, 1–4 (2005).
- [3] M. Bai, K. Knorr, M. J. Simpson, S. Trogisch, H. Taub, S. N. Ehrlich, H. Mo, U. G. Volkmann, and F. Y. Hansen, “Nanoscale observation of delayering in alkane films,” *Europhys. Lett.* **79**, 26003, 1–6 (2007).

## Studies of the Dynamics of Alkane Nanoparticles

S.-K. Wang<sup>1</sup>, M. Bai<sup>1</sup>, H. Taub<sup>1</sup>, J. R. D. Copley<sup>2</sup>, V. Garcia Sakai<sup>2</sup>, G. Gasparovic<sup>2</sup>, M. Rheinstädter<sup>1</sup>, U. G. Volkmann<sup>3</sup>, and F. Y. Hansen<sup>4</sup>

<sup>1</sup>*Department of Physics and Astronomy and University of Missouri Research Reactor, University of Missouri-Columbia, Columbia, MO 65211*

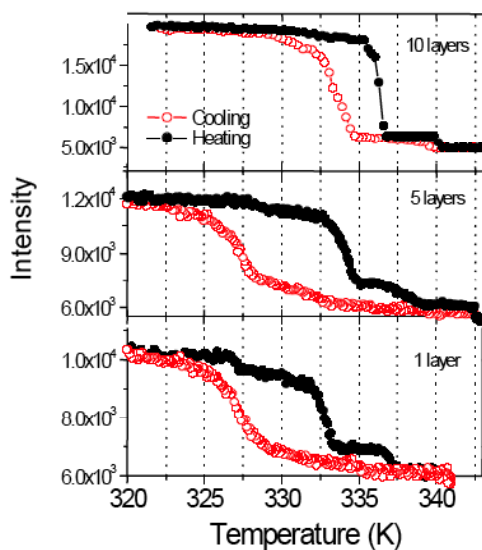
<sup>2</sup>*Center for Neutron Research, National Institute of Standards and Technology, Gaithersburg, MD 20899-8562*

<sup>3</sup>*Facultad de Física, Pontificia Universidad Católica de Chile – Santiago 22, Chile*

<sup>4</sup>*Department of Chemistry, Technical University of Denmark – IK 207 DTU, DK-2800 Lyngby, Denmark*

*E-mail: wangsi@missouri.edu*

Recently, we have been able to fabricate nanoparticles of intermediate-length alkane molecules ( $n\text{-C}_n\text{H}_{2n+2}$ ;  $20 < n < 40$ ) supported on  $\text{SiO}_2$ -coated  $\text{Si}(100)$  substrates. Our Atomic Force Microscopy [1] and synchrotron x-ray scattering [1,2] measurements indicate that these mesa-shaped particles have an orthorhombic structure in which the long molecular axis is aligned perpendicular to the  $\text{SiO}_2$  surface.



- (a) To investigate their dynamical properties, we have begun high-energy-resolution quasi-elastic neutron scattering measurements on dotriacontane ( $n = 32$ ) nanoparticles, using the High Flux Backscattering Spectrometer at NIST. As shown in Fig. 1, elastic scans (monochromator drive fixed) on three films of different size particles show previously unobserved step-like changes in intensity at the crystalline-to-rotator and rotator-to-fluid phase transitions [3]. They also suggest that sufficiently small nanoparticles might support a new rotator phase at 327 K [see Fig.1(c)], in addition to that which occurs in bulk [3].

Figure 1. Elastic intensity measured on heating and cooling of C32 nanoparticles with thickness equivalent to: (a) ~10 layers of perpendicular molecules; (b) ~5 layers; and (c) ~1 layer.

### References

- [1] M. Bai, K. Knorr, M. J. Simpson, S. Trogisch, H. Taub, S. N. Ehrlich, H. Mo, U. G. Volkmann, F. Y. Hansen, "Nanoscale observation of delayering in alkane films," *Europhys. Lett.* **79**, 26003, 1-6 (2007).
- [2] H. Mo, H. Taub, U. G. Volkmann, M. Pino, S. N. Ehrlich, F. Y. Hansen, E. Lu, and P. Miceli, "A novel growth mode of alkane films on a  $\text{SiO}_2$  surface," *Chem. Phys. Lett.* **377**, 99-105 (2003).
- [3] E. B. Sirota, H. E. King, Jr., D. M. Singer, and Henry H. Shao, "Rotator phases of the normal alkanes: an x-ray scattering study," *J. Chem. Phys.* **98**, 5809-5824 (1993).

# Temperature Dependent Dielectric Function of $\text{Al}_{0.52}\text{In}_{0.48}\text{P}$ and $\text{Ga}_{0.52}\text{In}_{0.48}\text{P}$

**E. Montgomery, T. Hofmann, and M. Schubert**

*Department of Electrical Engineering and Nebraska Center for Materials and Nanoscience, University of Nebraska-Lincoln, NE*  
*E-mail: emontgo1@bigred.unl.edu*

$(\text{Al}_x\text{Ga}_{1-x})_{0.52}\text{In}_{0.48}\text{P}$  is the work horse material for the optoelectronic devices grown lattice matched on GaAs. The device functionality and performance crucially depends on correct tailoring of alloy composition, lattice-mismatch-induced strain, long-range atomic ordering, and doping concentration, etc., which all affect the physical properties of the solid solution. Therefore, the optical in-situ monitoring and control of these parameters during the deposition of the epi-layers is a long term goal. This, however, requires precise knowledge of the optical properties of  $(\text{Al}_x\text{Ga}_{1-x})_{0.52}\text{In}_{0.48}\text{P}$  at growth temperatures which is currently is not exhaustive. Spectroscopic ellipsometry in the NIR to UV spectral range precisely measures the dielectric function and allows the determination of strain, composition, and ordering in  $(\text{Al}_x\text{Ga}_{1-x})_{0.52}\text{In}_{0.48}\text{P}$  [1,2].

Here, we report on an in-situ spectroscopic ellipsometry investigation of the temperature dependence of the dielectric function of  $\text{Al}_{0.52}\text{In}_{0.48}\text{P}$  and  $\text{Ga}_{0.52}\text{In}_{0.48}\text{P}$  in the temperature interval from room temperature to 500 °C. The epi-layers were grown lattice matched on GaAs substrate by metal-organic vapor phase deposition. The ellipsometric spectra are analyzed using a three-phase model (ambient-epilayer-substrate). We employ Adachi's composite critical point model in order to parameterize the dielectric function of  $\text{Al}_{0.52}\text{In}_{0.48}\text{P}$  and  $\text{Ga}_{0.52}\text{In}_{0.48}\text{P}$  and report on the temperature dependence of critical point energies, amplitudes, and broadening parameters [3].

## References

- [1] H. Thompkins and E. A. Irene (Eds.) *Handbook of Ellipsometry*, William Andrew Publishing, Highland Mills, 2004.
- [2] M. Schubert, J.A. Woollam, G. Leibiger, B. Rheinländer, I. Pietzonka, T. Sass, and V. Gottschalch, *J. Appl. Phys.* **89**, 2025 (1999).
- [3] S. Adachi, T. Kimura, and N. Suzuki, *J. Appl. Phys.* **74**, 3435 (1993).

## Author Index

Adenwalla, S. .... 54, 76	Haider, H. .... 69
Albanesi, E. A. .... 75	Halloran, S. T. .... 53
Aryal, S. .... 35	Han, B. S. .... 52
Bai, J. .... 69	Hansen, F. Y. .... 80, 81
Bai, M. .... 54, 80, 81	Harmon, G. .... 31
Baruth, A. .... 54	He, S. .... 31
Belashchenko, K. D. .... 28, 29, 42, 58	He, X. .... 60
Billa, R. .... 76	Hetterich, M. .... 50
Binek, Ch. .... 47, 51, 59, 60	Hoang, T. B. .... 70, 71
Brandt, M. .... 78	Hofmann, T. .... 50, 78, 82
Brewer, J. R. .... 69, 72	Holloway, A. .... 34
Brown, E. .... 27	Hong, N. .... 76
Buckley, B. .... 49	Horner, M. L. .... 41
Burton, J. D. .... 30	Huang, W. .... 77
Caruso, A. N. .... 74	Ilie, C. C. .... 68
Cheung, C. L. .... 33, 69, 72, 77	Jackson, H. E. .... 70, 71
Ching, W. Y. .... 23, 35, 36, 37, 38	Jacobson, P. A. .... 68
Choi, K.-J. .... 71	Jagadish, C. .... 70
Choi, Y.-J. .... 71	Jang, S. .... 31
Copley, J. R. D. .... 81	Janicka, K. .... 61
Daniel, B. .... 50	Jaswal, S. S. .... 58, 59
DeMarco, M. .... 31	Jesse, S. .... 64
Deo, R. .... 72	Jiang, H. .... 15
Dobrovitski, V. V. .... 19	Johnston, J. T. .... 65
Dowben, P. A. .... 42, 68, 75	Joyce, H. J. .... 70
Driver, M. S. .... 74	Kalinin, S. V. .... 64
Duan, Ch.-G. .... 58, 59	Kim, C. .... 31
Ducharme, S. .... 54, 62, 63, 64, 65, 66	Kim, J. .... 62, 64, 65, 66
Eckhardt, C. J. .... 73	Kirby, R. .... 44, 46, 49
Enders, A. .... 17	Kiriranov, E. .... 67
Fiyala, Y. .... 75	Kiyozumi, S. .... 39
Flatté, M. E. .... 22	Knorr, K. .... 80
Galiy, P. .... 75	Koch, J. .... 32
Garcia Sakai, V. .... 81	Komesu, T. .... 75
Garg, A. .... 20	Korlacki, R. .... 65
Garvin, K. L. .... 69	Kraemer, K. .... 62
Gasparovic, G. .... 81	Lambrecht, W. R. L. .... 16
Ge, Z. .... 62, 65	Lee, K.-Y. .... 71
George, T. A. .... 45	Leighton, C. .... 42
Glasbrenner, J. K. .... 29	Li, G. .... 33
Goldhaber, A. S. .... 41	Li, Z. .... 45, 46
Graves, B. .... 31	Liang, L. .... 38
Grundmann, M. .... 78	Liou, S.-H. .... 52, 53
	Liu, J. .... 75
	Liu, J. P. .... 31
	Liu, J.-J. .... 56

## Author Index

Lorenz, M. ....	78	Schubert, M. ....	50, 78, 79, 82
Losovyj, Y. B. ....	42, 75	Sellmyer, D. J. ....	43, 45, 46, 48, 51
Lu, J. ....	33	Sham, L. J. ....	9
Lukashev, P. ....	57	Shield, J. ....	48
Makinistian, L. ....	75	Skomski, R. ....	43, 45, 51
Manno, M. ....	42	Smirl, A. L. ....	21
Mardana, A. ....	54	Smith, L. M. ....	70, 71
Mei, W.-N. ....	33, 34, 56, 69	Smith, R. W. ....	56
Michalski, S. ....	44, 49	Smith, S. ....	13
Miller, N. ....	31	Snodgrass, J. ....	55
Mishra, A. ....	70, 71	Sokolov, A. ....	67
Mohapatra, H. ....	73	Stephens, S. ....	66
Montgomery, E. ....	82	Sui, Y. ....	46
Mryasov, O. N. ....	30	Sun, Z.-G. ....	43
Mukherjee, T. ....	51	Takacs, J. M. ....	62, 65, 68
Mullen, K. ....	27	Tan, H. H. ....	70
Mumgaard, R. ....	49	Tang, J.-M. ....	22
Namavar, F. ....	69	Taub, H. ....	80, 81
Nicholl, L. ....	52	Titova, L. V. ....	70, 71
Ogasawara, K. ....	39	Tsymbal, E. Y. ....	30, 58, 59, 61
Ouyang, L. ....	37	Vajk, O. ....	14
Pappas, D. ....	52, 53	van Schilfgaarde, M. ....	28
Park, J.-G. ....	71	Vasquez, H. ....	66
Patterson, M. M. ....	48	Velev, J. P. ....	28, 30, 58, 61
Paul, D. K. ....	77	Volkman, U. G. ....	80, 81
Petukhov, A. G. ....	18, 75	Voora, V. M. ....	78
Polisetty, S. ....	47, 59	Wang, G. ....	69
Poudyal, N. ....	31	Wang, L. ....	42
Poulsen, M. ....	68	Wang, S.-K. ....	81
Priour Jr., D. J. ....	40	Wang, Yi. ....	60
Reddy, D. S. ....	68	Wang, Yong. ....	62
Redepenning, J. ....	67	Wei, X.-H. ....	43
Reding, N. ....	62	Westman, C. ....	31
Reece, T. ....	54, 63	Wisbey, D. ....	42
Rheinstädter, M. C. ....	24, 81	Wu, N. ....	42
Rho, H. ....	71	Wysocki, A. L. ....	28, 29
Rodriguez, B. ....	64	Xiao, J. ....	68
Roostaei, B. ....	27	Xu, Y. ....	45
Rosa, L. G. ....	68	Yakovkin, I. N. ....	68
Rui, X. ....	48	Yan, M. ....	45
Rulis, P. ....	36, 38	Yao, H. ....	35, 37
Russek, S. E. ....	53	Yarrison-Rice, J. M. ....	70, 71
Sabirianov, R. ....	30, 31, 32, 33, 34, 55, 57, 69	Yuan, L. ....	52, 53
Saenger, M. ....	50	Zeng, H. ....	31
Sahoo, S. ....	47, 51, 59, 60	Zeng, X. C. ....	33, 69
Schmidt, D. ....	79	Zhang, R. ....	52, 53
Schubert, E. ....	79	Zhao, H. ....	21



## NOTES



## NOTES





College of Arts and Sciences  
Department of Physics and Astronomy



*website: <http://www.unl.edu/ncmn/MSSC54>*